Title

HERC6 regulates STING activity in a sex-biased manner through modulation of LATS2/VGLL3 Hippo signaling.

Journal

iScience, 27(2)

Authors

Uppala, Ranjitha

Sarkar, Mrinal

Young, Kelly

et al.

Publication Date

2024-02-16

DOI

10.1016/j.isci.2024.108986

Peer reviewed

iScience

CellPress
OPEN ACCESS

Article

HERC6 regulates STING activity in a sex-biased manner through modulation of LATS2/VGLL3 Hippo signaling

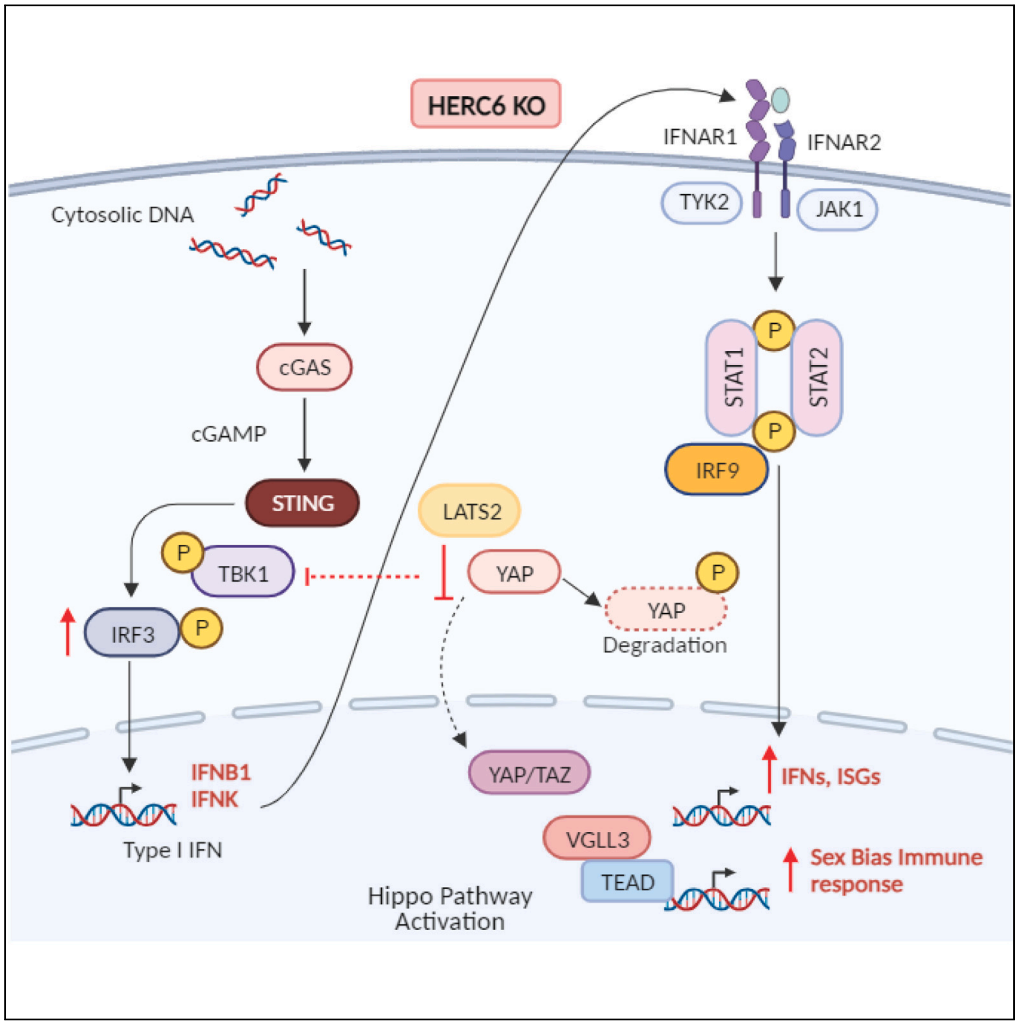

Ranjitha Uppala, Mrinal K. Sarkar, Kelly Z. Young, ..., Lam C. Tsoi, J. Michelle Kahlenberg, Johann E. Gudjonsson

johanng@med.umich.edu

Highlights

HERC6 is rapidly induced by type I interferons in human keratinocytes

HERC6 negatively regulates interferon responses to dsDNA but not to dsRNA stimuli

HERC6 ubiquitinates LATS2 and inhibits TBK1 to suppress STING pathway

HERC6 suppresses female-biased interferon responses in a VGLL3-dependent mechanism

Uppala et al., iScience 27, 108986
February 16, 2024
https://doi.org/10.1016/j.isci.2024.108986

iScience

CellPress
OPEN ACCESS

Article

HERC6 regulates STING activity in a sex-biased manner through modulation of LATS2/VGLL3 Hippo signaling

Ranjitha Uppala,[1,2] Mrinal K. Sarkar,[2] Kelly Z. Young,[2] Feiyang Ma,[2] Pritika Vemulapalli,[2] Rachael Wasikowski,[2] Olesya Plazyo,[2] William R. Swindell,[3] Emanual Maverakis,[4] Mehrnaz Gharaee-Kermani,[2,5] Allison C. Billi,[2] Lam C. Tsoi,[2] J. Michelle Kahlenberg,[5,6] and Johann E. Gudjonsson[2,5,6,7,*]

SUMMARY

Interferon (IFN) activity exhibits a gender bias in human skin, skewed toward females. We show that HERC6, an IFN-induced E3 ubiquitin ligase, is induced in human keratinocytes through the epidermal type I IFN; IFN-κ. HERC6 knockdown in human keratinocytes results in enhanced induction of interferon-stimulated genes (ISGs) upon treatment with a double-stranded (ds) DNA STING activator cGAMP but not in response to the RNA-sensing TLR3 agonist. Keratinocytes lacking HERC6 exhibit sustained STING-TBK1 signaling following cGAMP stimulation through modulation of LATS2 and TBK1 activity, unmasking more robust ISG responses in female keratinocytes. This enhanced female-biased immune response with loss of HERC6 depends on VGLL3, a regulator of type I IFN signature. These data identify HERC6 as a previously unrecognized negative regulator of ISG expression specific to dsDNA sensing and establish it as a regulator of female-biased immune responses through modulation of STING signaling.

INTRODUCTION

Females have heightened type I interferon (IFN) activity compared to males. Hyperactive IFN responses are a characteristic feature of systemic lupus erythematosus (SLE), leading to aberrant innate and adaptive immune activation that often precedes the clinical manifestation of the disease.[1] Clinically, SLE predominantly affects women, with women outnumbering men 9:1.[2] However, the cause of this sex discrepancy is inadequately explained by environmental factors or sex hormones.[2] Although there is a shared pattern of increased type I IFN activity and sex bias observed in multiple autoimmune diseases, the relationship between the two remains unclear.[2]

The role of the skin is well established to play a key role in SLE pathogenesis. Skin manifestations are common in SLE,[3] and the skin is a frequent trigger of SLE flares, particularly following exposure to UV irradiation.[4] We have recently demonstrated that photosensitivity in SLE is closely linked to interferon kappa (IFN-κ), a type I IFN derived from keratinocytes.[5] A critical regulator of IFN-κ expression in keratinocytes depends on the activity of the cyclic GMP-AMP synthase (cGAS)—stimulator of interferon genes (STING) pathway,[6] a sensor of foreign DNA.[7] Cytosolic DNA sensing by STING has been shown to occur in lupus keratinocytes.[8] Through phosphorylation of TANK-binding kinase 1 (TBK1) and interferon regulatory factor 3 (IRF3),[9,10] it leads to the induction of interferon-stimulated genes (ISGs) expression that is prominent in lupus keratinocytes and has been shown to correlate with disease severity.[11] Many of these ISGs encode proteins with antiviral properties,[12,13] with some acting back on STING to further amplify its responses.[14] The molecules are thought to involve positive feedback regulation via STAT1 promoter binding,[14] ubiquitination,[15] sumoylation,[16] phosphorylation,[17] methylation,[18] or[19] acetylation of cGAS or STING itself.

HERC is an evolutionarily conserved family of E3 ubiquitin ligases comprising six family members, HERC1-6, and the divergent expression patterns of HERCs in tissues likely reflect their functional diversity.[20] HERC6 is under strong and recurrent adaptive evolution in mammals, likely reflective of its potential role in immune responses to viral pathogens.[20] Consistent with this notion of a role in immune responses, HERC6 induction has been reported in COVID-19-infected tissues[21] and was recently shown to be a biomarker of SLE.[22] Notably, HERC6 functions are distinct in humans versus mice. For example, Mouse Herc6 has been reported to be functionally similar to human HERC5,[23] and no

[1]Graduate Program in Immunology, University of Michigan, Ann Arbor, MI 48109, USA
[2]Department of Dermatology, University of Michigan, Ann Arbor, MI 48109, USA
[3]Department of Internal Medicine, University of Texas Southwestern Medical Center, Dallas, TX 75390, USA
[4]Department of Dermatology, University of California, Davis, Davis, CA 95616, USA
[5]Department of Internal Medicine, University of Michigan, Ann Arbor, MI 48109, USA
[6]A. Alfred Taubman Medical Research Institute, Ann Arbor, MI 48109, USA
[7]Lead contact
*Correspondence: johanng@med.umich.edu
https://doi.org/10.1016/j.isci.2024.108986

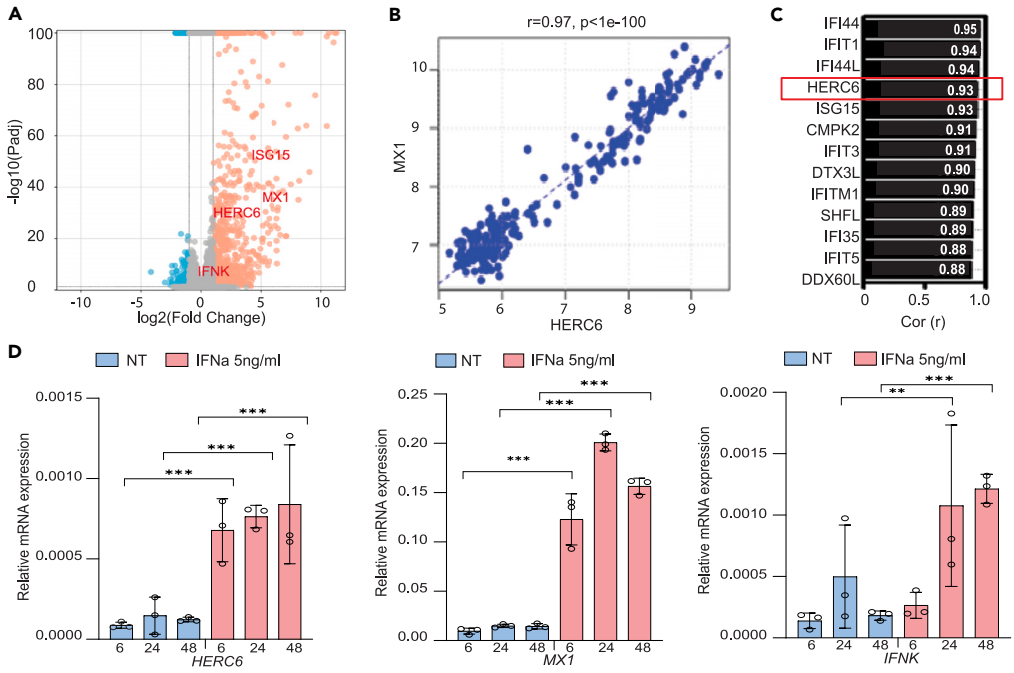

Figure 1. HERC6 is an interferon stimulated gene (ISG)

(A) Volcano plot showing 1,582 upregulated and 585 down-regulated genes with IFN-α stimulation in primary human keratinocytes (FDR<0.05).

(B) HERC6 expression correlation analysis with MX1 from primary human keratinocytes.

(C) *MX1* correlated genes in primary human keratinocytes upon IFN-α stimulation.

(D) Gene expression analysis of IFN-α stimulated N/TERT keratinocytes at indicated time points (Mean ± SEM, p < 0.001 = ***, p < 0.01 = **, p < 0.05 = *, ns = not significant, Student's t test, n = 3) Assume that NT = no treatment group.

clear homolog to human HERC6 has been identified in mice, restricting functional testing of HERC6 to human cells and tissues. More importantly, there has not been any previous research examining the function of HERC6 in keratinocytes, and in relation to exogenous stimuli.

Numerous studies demonstrate that type I IFN responses are stronger in women, conferring protection against viral infections than men. However, most of these studies were conducted using research focused on plasmacytoid dendritic cells, a major source of IFN alpha (IFN-α),[24] and in the context of TLR7.[25,26] Whether STING signaling has a role in sex-biased immune responses has not been previously reported.

Herein, we demonstrated the interactions between STING, IFN signaling, and HERC6 in epithelial keratinocytes, a major source of the type I IFN-κ. We demonstrated that HERC6 is an ISG that acts through the ubiquitination of LATS2, a kinase of the Hippo signaling pathway, to modulate STING activation. This modulation of STING activation is sex-biased and VGLL3-dependent, establishing HERC6 as a suppressor of female-biased immune responses induced by STING activation.

RESULTS

HERC6 is rapidly induced by type I IFNs in keratinocytes

We analyzed RNA-sequencing data of IFNα-stimulated primary human keratinocytes. We found that *HERC6* expression was rapidly upregulated (FDR <0.05) by IFNα and positively correlated with type I ISGs in primary human keratinocytes, including *MX1*, *IFNK*, and *ISG15* (Figure 1A). Notably, *HERC6* was one of the top 5 genes that correlated with *MX1*, a well-known ISG,[27] with a correlation coefficient of r = 0.97 (*MX1*) and r = 0.98 (*OAS2*) (Figures 1B, 1C, and S1A). *HERC6* induction occurred rapidly within 6 h of IFNα-stimulation (Figure 1D). These data demonstrate that HERC6 is an ISG in keratinocytes.

HERC6 negatively regulates IFN response to dsDNA but not to dsRNA stimuli

To determine if HERC6 plays a role in the activation of type I IFN responses, we stimulated control or *HERC6* knockdown (KD) primary human keratinocytes with or without the STING agonist, cyclic GMP-AMP (cGAMP), or the TLR3 agonist polyinosinic: polycytidylic acid (Poly(I:C)). Both STING and TLR3 activation resulted in the expression of ISGs (Figure 2A), including *HERC6*, in control cells (Figure S2A). However, siRNA targeting of *HERC6* (>85% KD efficiency as shown in Figure S2A), resulted in increased ISG responses to cGAMP but not to Poly(I:C) (Figure 2A). Notably, no significant changes were observed in ISG expression following cGAMP stimulation with HERC6 knockdown (KD) in primary human fibroblasts that express STING (Figures S2B–S2D), demonstrating that HERC6 KD regulation is specific to keratinocytes. To confirm the regulatory effects of HERC6 on ISGs, we employed a stable MX1 reporter line in keratinocytes, where *MX1* transcriptional activity is reported by GFP expression with IFNα-stimulation (Figure 2B). As expected, GFP expression in the MX1-GFP reporter was higher in

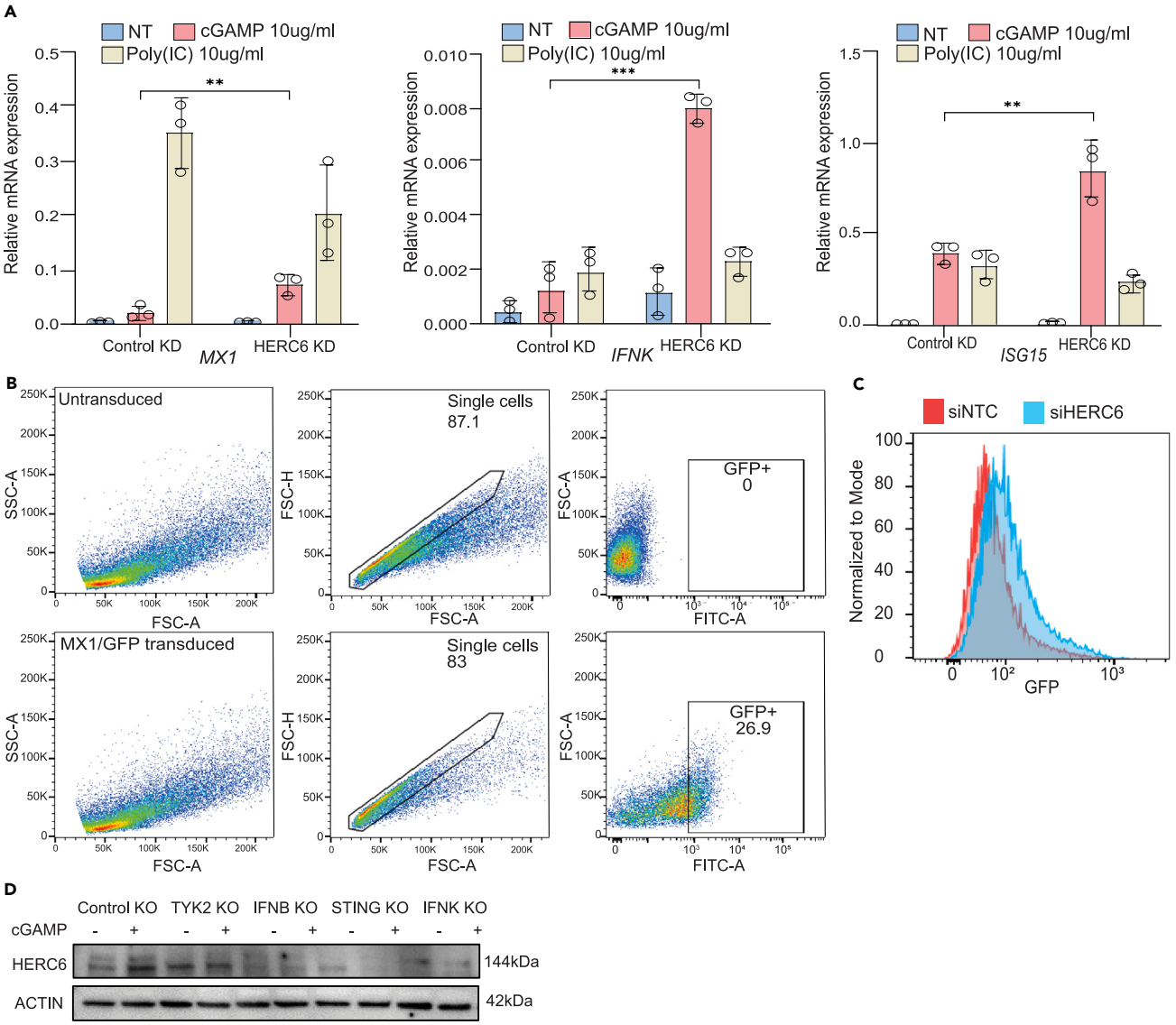

Figure 2. HERC6 negatively regulates type I interferon activity in cGAMP-stimulated keratinocytes

(A) Gene expression analysis of cGAMP or Poly(I:C) stimulated control or HERC6 knockdown primary human keratinocytes (Mean ± SEM, $p < 0.001$ = ***, $p < 0.01$ = **, $p < 0.05$ = *, ns = not significant, Student's t test, n = 3). Assume that NT = no treatment group.

(B) Gating strategy to sort GFP expressing single cells (GFP+) after IFN-α stimulation for 24 h in untransduced or MX1/GFP transduced keratinocytes.

(C) Histogram representing GFP expression in MX1/GFP reporter with control (siNTC) or HERC6 (siHERC6) knockdown.

(D) Western blot analysis of HERC6 in indicated knockout keratinocytes.

HERC6 KD compared to the control cells (Figure 2C). To determine whether HERC6 expression is dependent on IFN or STING activity in keratinocytes, we assessed HERC6 levels and ISG expression in *TYK2*, *IFNK*, *TMEM173 (STING protein)*, and *IFNB1* knockout (KO) keratinocytes. HERC6 was significantly decreased at the transcript level and absent in *TYK2*, *IFNB1*, *STING*, and *IFNK* KO keratinocytes (Figures 2D and S2E). Interestingly, cGAMP responses were suppressed in *TYK2*, *IFNB1*, and *IFNK* KO lines and absent in *TMEM173* KO keratinocytes (Figures 2F and 2G), demonstrating the dependency of HERC6 on autocrine type I IFN activity, which is absent in fibroblasts,[5] and STING activation. These findings indicate that HERC6 requires STING-dependent IFN-k activity for its expression and function.

HERC6 knockout amplifies IFN signaling in keratinocytes

To address the role of HERC6 in keratinocytes, we generated *HERC6* KO using CRISPR/Cas9 in N/TERT cells as previously described.[5] A 23 bp deletion in *HERC6* exon1 region was confirmed by Sanger sequencing, western blotting, and RT-qPCR analysis (Figures 3A and S3A). Consistent with the findings from HERC6 KD (Figure 2A), *HERC6* KO resulted in amplified expression of *IFNK* and other ISGs upon cGAMP

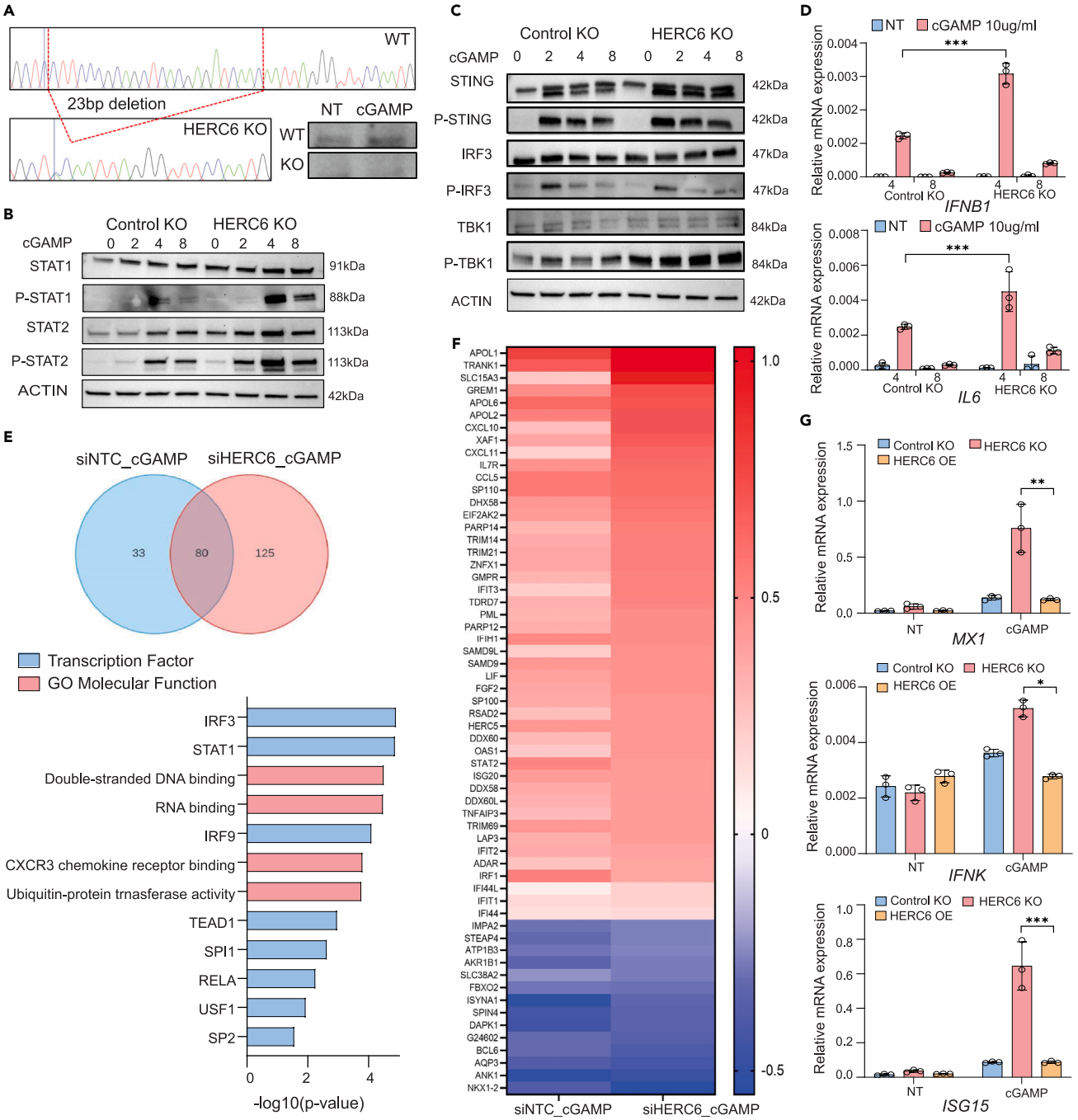

Figure 3. HERC6 knockout keratinocytes have sustained STING-TBK1 signaling amplifying type I IFN responses

(A) Sanger sequencing of exon1 and western blot analysis of *HERC6* knockout keratinocytes generated using CRISPR/Cas9 in N/TERT cells.

(B) Western blot analysis of type I interferon-related genes in cGAMP stimulated control or *HERC6* knockout keratinocytes at indicated time points in hours.

(C) Western blot analysis of STING pathway-related genes in cGAMP stimulated control or *HERC6* knockout keratinocytes at indicated time points in hours.

(D) Gene expression analysis for STING-induced genes in control or *HERC6* knockout keratinocytes (Mean ± SEM, $p < 0.001$ = ***, $p < 0.01$ = **, $p < 0.05$ = *, ns = not significant, two-way ANOVA, n = 3). Assume that NT = no treatment group.

(E) (Top) Venn diagram showing the total number of genes differentially regulated in non-targeting control (siNTC) or *HERC6* (*siHERC6*) knockdown keratinocytes with cGAMP stimulation (FDR <0.05, n = 3 males and 3 females; (Bottom) GO terms of 80 DEGs that overlap between control and HERC6 knockdown keratinocytes for transcription factors in blue and molecular function in coral.

(F) Heatmap representing dysregulated genes in log2 fold change in control or *HERC6* knockdown primary human keratinocytes with cGAMP stimulation (n = 6).

(G) Gene expression analysis of ISGs in un-treated (NT) or CGAMP treated control KO, *HERC6* KO and HERC6 OE keratinocytes (Mean ± SEM, $p < 0.001$ = ***, $p < 0.01$ = **, $p < 0.05$ = *, ns = not significant, Student's t test, n = 3).

stimulation (Figure S3B). In addition, we observed a persistent elevation in type I IFN signaling in cGAMP-stimulated *HERC6* KO keratinocytes, as evidenced by the upregulation of STAT1, phosphor (p)-STAT1, STAT2, and p-STAT2 (Figure 3B).

Amplification of IFN responses secondary to loss of HERC6 is due to increased STING-TBK1 activity

Consistent with increased STING activity in *HERC6* KO keratinocytes, we observed increased levels of p-STING, p-IRF3, and p-TBK1 with cGAMP stimulation in *HERC6* KO compared to control KO keratinocytes (Figures 3C and S3C). The effect on IFN signaling was seen as early as 2 h following cGAMP treatment as shown by increased P-STAT2 in *HERC6* KO keratinocytes and after 4 and 8 h cGAMP treatment on STING-TBK1 signaling (Figures 3B and 3C), suggesting that the increased ISG response is secondary to STING activation. In line with these findings, *HERC6* KO keratinocytes demonstrated increased expression of *IFNB1* and *IL6* by RT-qPCR (Figure 3D). Thus, *HERC6* KOs exhibited a difference in IFN and STING signaling compared to control, with higher levels of p-STAT2 and *p*-TBK1, even in the absence of stimulation (Figures S4A and S4B). These responses were primarily STING-driven; we examined the effects of STING knockdown by siRNA. We observed that knockdown of STING attenuated the elevated expression of *IFNB1* and *IL6* in *HERC6* KO keratinocytes (knockdown efficiency >90% as shown in Figure S4C). Both STING and HERC6 were increased in the cytoplasm after cGAMP stimulation (Figure S4D).

To determine the broader effect of HERC6 on STING activation, we performed bulk RNA sequencing of non-targeting control (siNTC) or *HERC6* KD (*siHERC6*) primary human keratinocytes with or without cGAMP stimulation. Using a threshold of false-discovery rate (FDR) < 0.05, we assessed the number of differentially expressed genes (DEGs). *HERC6* KD keratinocytes had an increased number of DEGs compared to control with 80 DEGs in common (Figure 3E). Gene ontology (GO) terms for the 80 shared DEGs were enriched for targets of transcription factors, including IRF3, STAT1, TEAD1, RELA, and molecular functions related to innate immune response including DNA and RNA binding, CXCR3 chemokine receptor binding and ubiquitin-protein transferase activity in *HERC6* KD keratinocytes (Figure 3E). Several ISGs including *OAS1*, *STAT2*, *XAF1*, and *IFIT3* were upregulated in cGAMP-stimulated *HERC6* KD keratinocytes compared to cGAMP-stimulated control (Figure 3F), with *HERC6* KD having an overall broader and stronger impact compared to control KD keratinocytes (Figure S4E). Conversely, HERC6 over-expressing (OE) keratinocytes attenuated ISG responses to cGAMP stimulation (Figures 3G and S4F).

These data demonstrate that *HERC6* negatively regulates type I IFN activity by modulating STING-TBK1 signaling.

cGAMP stimulation resulted in enhanced LATS2 activity in *HERC6* KO keratinocytes

HERC6 has been reported to bind to LATS2,[28] a serine/threonine protein kinase that regulates the Hippo signaling pathway through phosphorylation of YAP1 for cytosolic sequestration.[29] Intriguingly, TEAD1, a transcription factor downstream of the Hippo signaling pathway,[30] is significantly affected by *HERC6* KD (Figure 3E). To assess the relationship between HERC6 and LATS2 function, we first determined *LATS2* mRNA expression by QRT-PCR in control or *HERC6* KO keratinocytes with or without cGAMP. We observed increased *LATS2* mRNA expression in cGAMP-stimulated *HERC6* KO keratinocytes compared to the control (Figure 4A), which was also validated in our bulk RNA-seq data from *HERC6* KD primary human keratinocytes (Figure S5A). These findings were validated on the protein level by western blotting. In addition, increased and sustained total and p-LATS1/2 levels were observed in *HERC6* KO with cGAMP stimulation (Figures 4B and S5B).

The increased STING/TKB1 activity with loss of HERC6 is LATS2 dependent

To determine the role of LATS2 in modulating the increased STING/TBK1 activity observed with the loss of HERC6, we used siRNA targeting *LATS2* (KD efficiency >75% as shown in Figure 5C), which attenuated ISG responses in *HERC6* KOs (Figure 4C). To assess the levels of YAP1, we performed fractioned western blot analyses of the cytosolic and nuclear fractions of both control and *HERC6* KO with or without cGAMP stimulation. This demonstrated a reduction in cytosolic and nuclear YAP1 levels in *HERC6* KO keratinocytes (Figure 4D). The observed reduction in cytosolic YAP1 levels led us to hypothesize that YAP1 undergoes increased degradation. To examine this, we inhibited total proteasomal degradation using the proteasomal inhibitor MG132 [31]. MG132, alone or with cGAMP treatment, led to increased YAP1 levels in *HERC6* KO, suggesting that the decrease in YAP1 levels is due to increased YAP1 proteasomal degradation (Figures 4E and 4F). These data indicate that increased LATS2 activity in *HERC6* KO keratinocytes increases YAP1 degradation.

HERC6 ubiquitinates LATS2 resulting in increased TBK1 activity

TRULI is a small molecule inhibitor of LATS2 kinase activity.[31] To validate increased LATS2 activity in *HERC6* KO keratinocytes, we inhibited LATS2 using TRULi. LATS2 inhibition resulted in decreased expression of ISGs (Figure 5A), consistent with what we observed with *LATS2* KD in *HERC6* KO keratinocytes (Figure 4C). Consistent with the role of YAP1 acting as inhibitors of TBK1/STING activation, increased TBK1 expression was observed in *HERC6* KO with cGAMP activation (Figure 5B), and pTKB1 (Figure 5C), which was suppressed with TRULI in cGAMP-stimulated *HERC6* KO (Figure 5C). These data indicate that LATS2-mediated YAP1 degradation increases TBK1 activation in *HERC6* KO keratinocytes.

As HERC6 belongs to a family of E3 ubiquitin ligases,[32] we examined whether HERC6 regulated LATS2 through ubiquitination. We performed ubiquitin conjugates immunoprecipitation followed by a pull-down of LATS2 in empty (PCMV6) or *HERC6*-transfected HEK293 cells. LATS2 was ubiquitinated to a higher degree in HERC6-*transfected* cells compared to empty vector-transfected cells (Figure 5D). Furthermore, HERC6 and LATS2 colocalized in the cytoplasm upon cGAMP treatment (Figure 5E). These results indicate that HERC6 regulates STING activation through the ubiquitination of LATS2, which, in turn, inhibits TBK1 through increased YAP1, thereby suppressing STING activation.

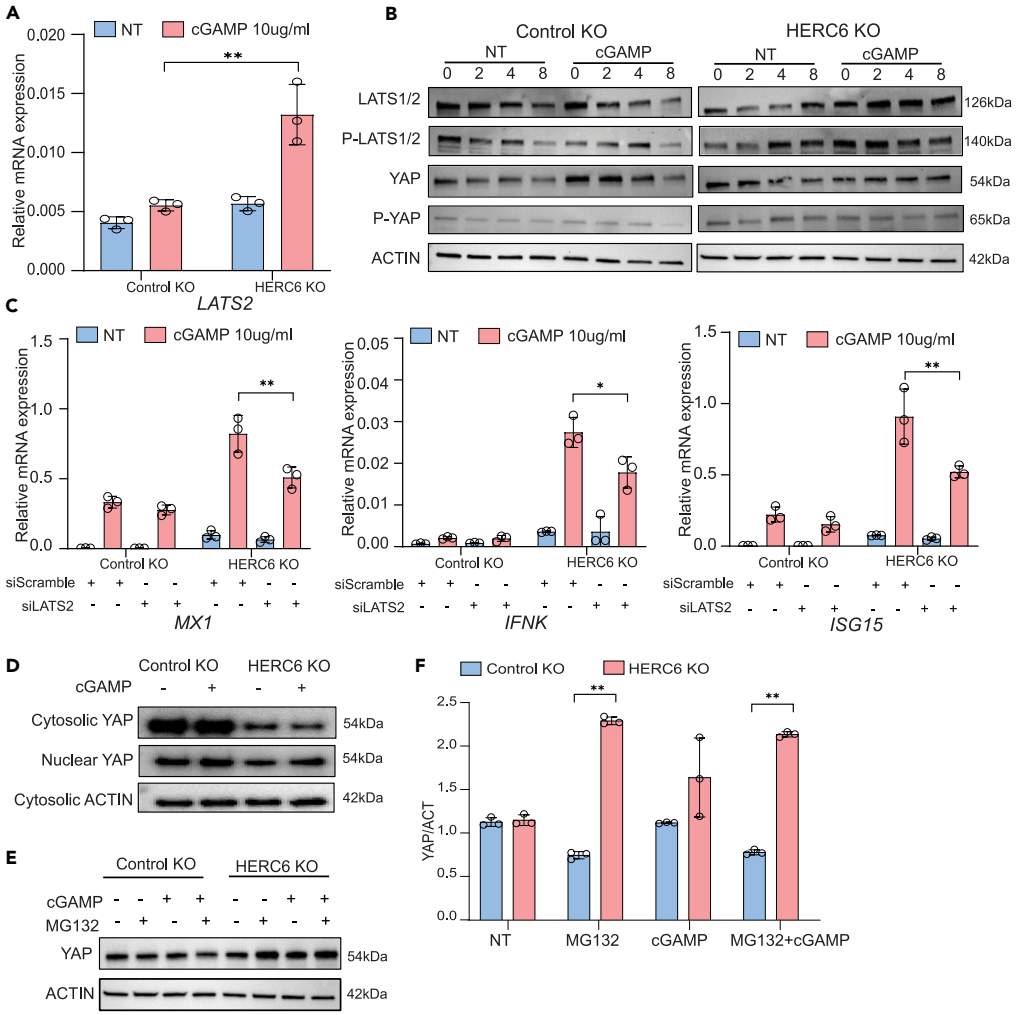

Figure 4. HERC6 knockout keratinocytes have increased LATS2 activity promoting increased YAP1 degradation

(A) LATS2 gene expression in control or *HERC6* knockout keratinocytes after cGAMP stimulation (Mean ± SEM, $p < 0.001$ = ***, $p < 0.01$ = **, $p < 0.05$ = *, ns = not significant, Student's t test, n = 3). Assume that NT = no treatment group.

(B) Western blot analysis of LATS2 and YAP1 in cGAMP stimulated control or in *HERC6* knockout keratinocytes at indicated time points in hours. Assume that NT = no treatment group.

(C) Gene expression analysis of cGAMP stimulated control or *HERC6* knockout keratinocytes with or without *LATS2* knockdown (Mean ± SEM, $p < 0.001$ = ***, $p < 0.01$ = **, $p < 0.05$ = *, ns = not significant, one-way ANOVA, n = 3). Assume that NT = no treatment group.

(D) Western blot analysis of cytosolic and nuclear YAP1 in control or *HERC6* knockout keratinocytes.

(E) Western blot analysis of YAP1 in cGAMP stimulated control or *HERC6* knockout keratinocytes and with or without proteasomal inhibitor, MG132.

(F) Quantification of western blot from Figure 4E representing normalized relative band intensity of YAP (Mean ± SEM, $p < 0.001$ = ***, $p < 0.01$ = **, $p < 0.05$ = *, ns = not significant, one-way ANOVA, n = 3). Assume that NT = no treatment group.

HERC6 suppressed female-biased STING responses through a VGLL3-dependent mechanism

While there was no difference in *HERC6* mRNA expression between primary keratinocytes from healthy males and females (Figure 6A), we observed greater *HERC6* mRNA induction upon cGAMP stimulation in female SLE keratinocytes compared to healthy male or female keratinocytes (Figure 6B). Notably, ISG responses upon cGAMP stimulation were robustly amplified in female compared to male keratinocytes with *HERC6* KD (Figures 6A and 6C). To identify the mechanisms involved in this sex bias, we used primary SLE keratinocytes which exhibit female-biased IFN responses. We used cGAMP-stimulated female SLE keratinocytes along with siRNAs against *HERC6* and *VGLL3*, a transcriptional co-factor previously implicated in sex-biased immune responses[33] and a regulator of Hippo signaling activity.[34] We observed increased VGLL3 in *HERC6* KD female keratinocytes compared to male keratinocytes (Figures 6B and 6D–6F), The knockdown efficiency for both *HERC6* and *VGLL3* in lupus keratinocytes was robust (Figure 6D), and KD of both *VGLL3* and *HERC6* together attenuated heightened ISG activity (Figure 6C). Consistent with these findings, analysis of bulk RNA-seq data from cGAMP stimulated primary human female, and male keratinocytes demonstrated that *HERC6* KD was associated with greater enrichment for

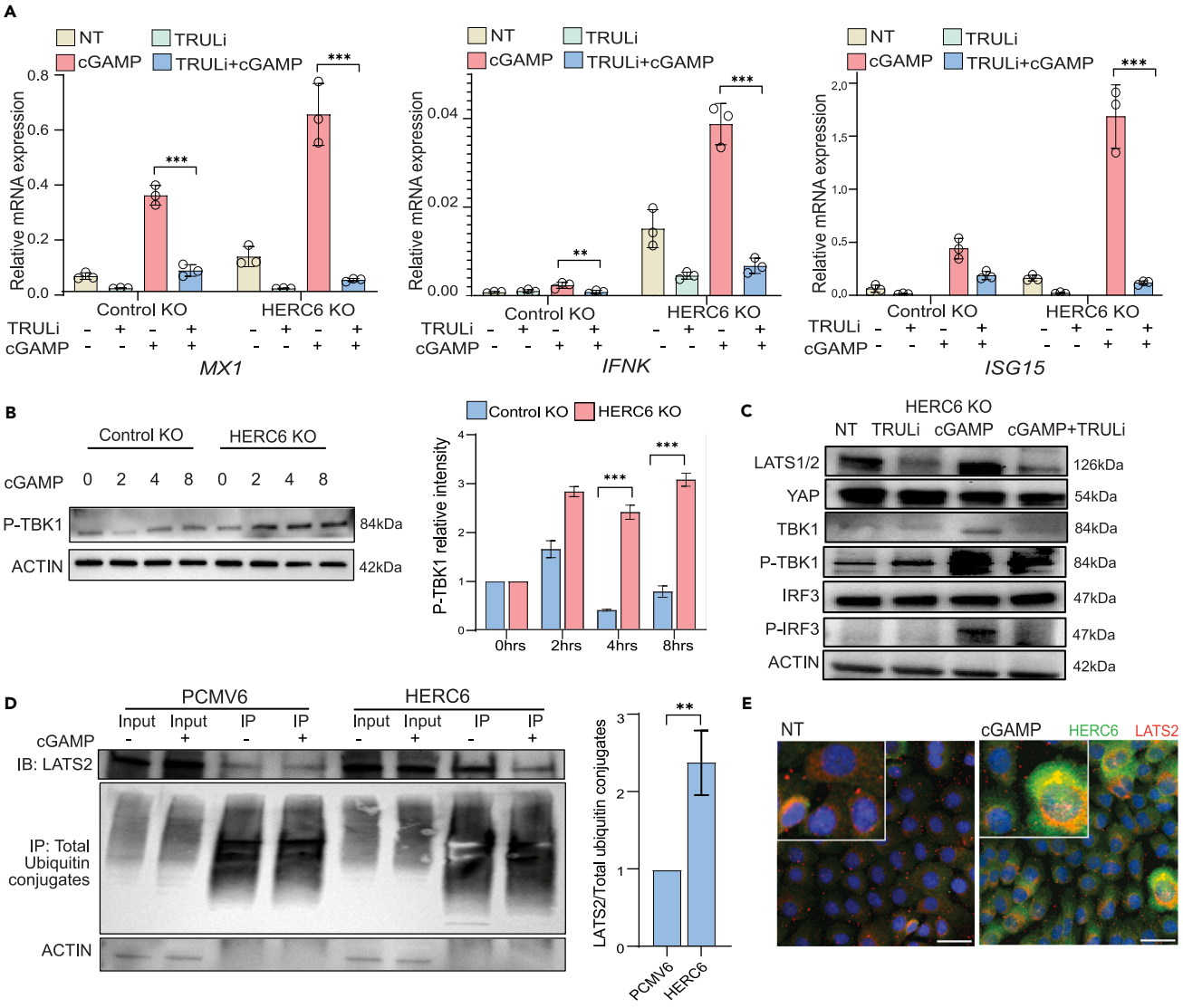

Figure 5. HERC6 carries out LATS2 ubiquitination to further induce TBK1-STING activation

(A) Gene expression analysis of ISGs upon LATS2 inhibition using TRULI in cGAMP stimulated control or *HERC6* KO keratinocytes (Mean ± SEM, $p < 0.001$ = ***, $p < 0.01$ = **, $p < 0.05$ = *, ns = not significant, two-way ANOVA, n = 3).

(B) Western blot analysis of P-TBK1 (*on the left*) and relative quantification (*on the right*) in cGAMP stimulated control or *HERC6* knockout keratinocytes.

(C) Western blot analysis of LATS2, YAP1, TBK1, P-TBK1, IRF3, and P-IRF3 in cGAMP stimulated *HERC6* knockouts with TRULI treatment.

(D) Western blot analysis (*on the left*) of ubiquitin conjugates immunoprecipitation pull-down of empty (PCVM6) or HERC6 transfected HEK293 cells and relative quantification (*on the right*).

(E) Confocal image analysis of control knockouts with or without cGAMP (HERC6 in green, LATS2 in red, and DAPI nuclear staining in blue).

GO terms associated with IFN responses and cytosolic sensing of foreign DNA in female keratinocytes (Figure 6G). Furthermore, the total number of differentially expressed genes (DEGs) was increased in both unstimulated and cGAMP-stimulated female compared to male keratinocytes, consistent with more robust ISG responses with HERC6 KD (Figure 6D). These findings show that HERC6 suppresses ISG responses by modulation of VGLL3-dependent Hippo pathway signaling in female keratinocytes. This suggests that HERC6 may be responsible for dampening female-biased immune responses through modulation of STING activity (Figure 6E).

DISCUSSION

Here, we demonstrated that HERC6, an E3 ubiquitin ligase, is rapidly induced in epidermal keratinocytes upon IFN-α stimulation or by nucleotide sensing mechanisms to either dsDNA or dsRNA and dependent on STING and autocrine IFN-κ activity. Notably, the suppressive role of

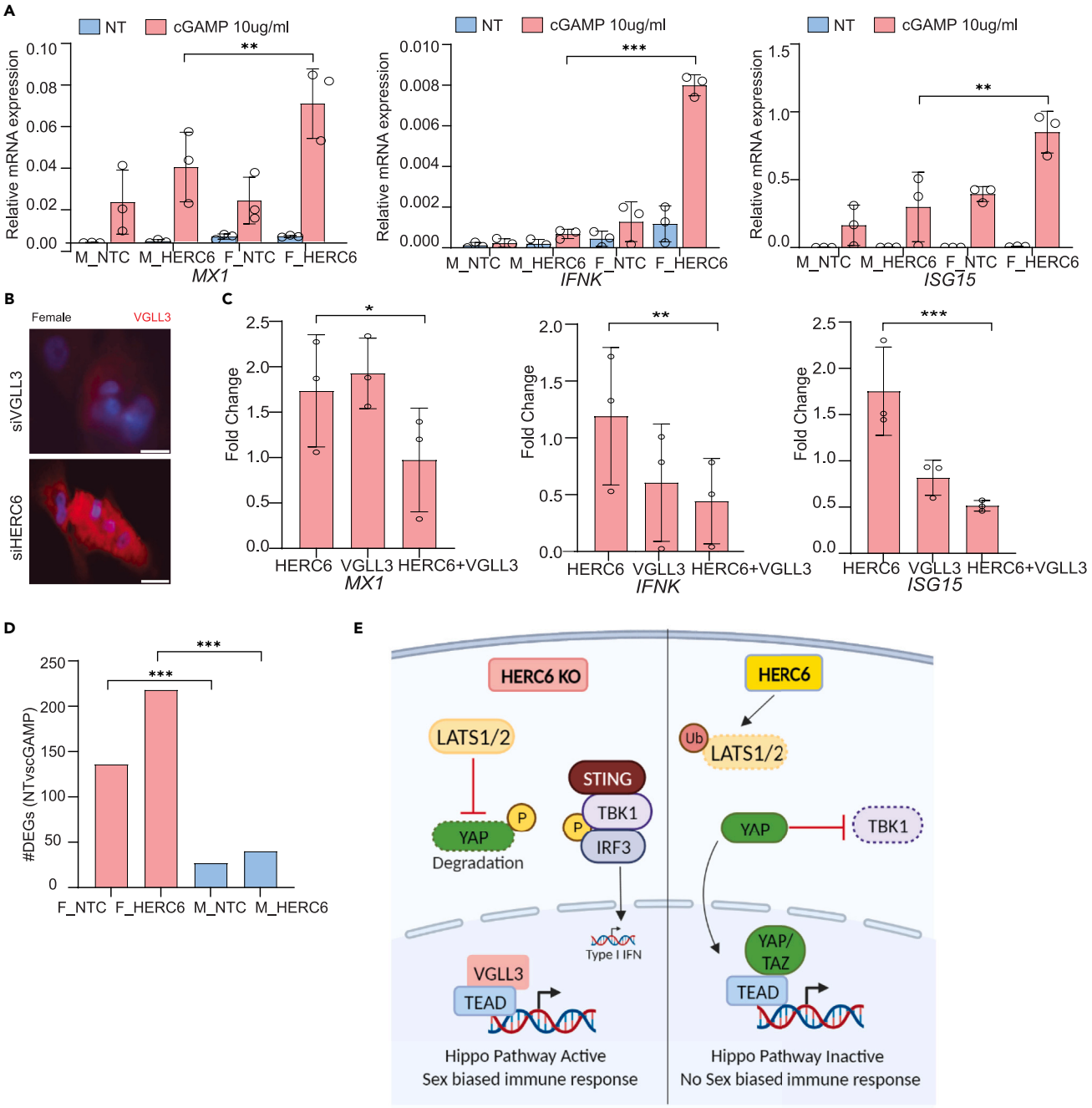

Figure 6. HERC6 suppresses cGAMP-dependent sex-biased interferon responses in lupus keratinocytes in a VGLL3-dependent manner

(A) Interferon-stimulated gene expression in normal male (M) or normal female (F) keratinocytes with control (NTC) or HERC6 (HERC6) knockdown and with or without cGAMP stimulation (Mean ± SEM, $p < 0.001$ = ***, $p < 0.01$ = **, $p < 0.05$ = *, ns = not significant, two-way ANOVA, n = 3).

(B) Immunofluorescence staining of VGLL3 in primary human female keratinocytes with VGLL3 or *HERC6* knockdown (VGLL3 in red and DAPI nuclear staining in blue).

(C) Gene expression analysis representing fold change compared to knockdown of non-targeting control (NTC) of *HERC6*, *VGLL3*, or both *HERC6+VGLL3* in non-lesional female lupus keratinocytes (Mean ± SEM, $p < 0.001$ = ***, $p < 0.01$ = **, $p < 0.05$ = *, ns = not significant, ordinary one-way ANOVA fold-change relative to control knockdown, n = 3).

(D) Total number of DEGs in female or male control knockdown (siNTC) or *HERC6* knockdown keratinocytes with cGAMP stimulation.

(E) Schematic illustrating the mechanism involving sex-biased IFN responses in HERC6 KO keratinocytes through modulation of VGLL3 Hippo pathway.

HERC6 on cGAMP signaling was specific to epidermal keratinocytes and not seen in fibroblasts and acted through modulation of the LATS2/TBK1/VGLL3 Hippo-pathway to suppress female-biased immune responses.

Our data are consistent with a significant role for HERC6 as a modulator of the STING pathway, particularly in disease states such as systemic lupus erythematosus (SLE), characterized by a prominent sex-biased type I IFN activity.[1] This modulation of STING activation is through ubiquitination of LATS2 kinase upon sensing dsDNA agonist. The ubiquitination of LATS2 results in decreased LATS2 activity, likely through increased proteasomal degradation of LATS2, increasing YAP1, which in turn promotes inhibition of TBK1, resulting in suppression of downstream IRF3-dependent signaling from STING. Conversely, decreased levels of HERC6 lead to increased degradation of YAP1, effectively decreasing both cytoplasmic and nuclear levels of YAP1, leading to decreased competition in binding to TEADs transcription factors with nuclear transcription co-factors, such as VGLL3,[35] shifting the binding toward increased VGLL3:TEAD activity, thereby amplifying VGLL3 responses. As VGLL3 is primarily located in the nucleus of female keratinocytes, this shift likely only occurs in women to amplify IFN responses. This aligns with our previous findings describing VGLL3, a modulator of Hippo-signaling, as a master regulator of sex-biased immune responses.[36] A crosstalk between the Hippo-STING signaling pathways has been described previously,[37,38] and LATS1/2 deletion has been shown to enhance type I IFN response in melanoma cells.[39] However, sex-specific regulation of immune responses through modulation of STING activation has not been previously reported.

SLE is a female-biased disease characterized by heightened type I IFN responses.[1,2] Although there is a trend for the peak of high type I IFN activity being earlier in female patients, there are no significant quantitative differences in type I IFN activity between male and female SLE patients once the disease state is fully established.[40] Female-biased type I IFN responses have been reported in plasmacytoid dendritic cells (pDCs) from healthy individuals responding to TLR7 or TLR9 ligands.[41] Still, interestingly pDCs are markedly diminished in inflamed SLE skin,[42] and have also been described to have lost their effector capacity.[43] These findings suggest that while there may be sex-specific differences at baseline in type I IFN responses between men and women, these differences are balanced once the disease process is established. These underlying female-biased responses are unmasked and amplified in the absence of HERC6, suggesting that HERC6 is a suppressor of female-specific immune responses through the modulation of STING responses. This role of HERC6 may extend beyond the skin, as differential expression of HERC6 has been reported in SLE PBMCs and glomeruli of lupus nephritis patients.[44,45]

While we did not find evidence for the involvement of HERC6 in TLR3 responses, which is a sensor of intracellular double-stranded RNA (dsRNA),[46] we did not address the potential role(s) of HERC6 on TLR7 or TLR9 pathways, both of which have been previously implicated in sex-biased immune responses.[47,48] Notably, though, TLR3 stimulation through Poly(I:C) was a more potent inducer of HERC6 expression than stimulation with the STING agonist cGAMP, suggesting that HERC6 might have a role in cross-regulation between TLR3 and STING signaling, but this will need to be addressed in future studies.

Our findings have major implications regarding our understanding of STING signaling and sex-biased immune responses and emphasize the role of the Hippo pathway through modulation of HERC6-STING activity as a critical circuit in the modulation of autoimmune diseases such as SLE.

Limitations of the study

There are certain limitations inherent to our study. We did not explore the mechanistic significance of STING activity via Hippo pathway modulation in cell types other than human keratinocytes. This was due to the lack of observable changes in ISG activity upon HERC6 knockdown in HEK293 cells and human fibroblasts. While a humanized HERC6 animal model would have provided valuable insights, we restricted our experiments to human keratinocytes given the significance of HERC6 in human physiology. Moreover, our investigation did not delve into the role of HERC6 in regulating the STING pathway in other autoimmune diseases. Our future research endeavors will focus on examining VGLL3-dependent sex-biased IFN responses in autoimmune skin conditions such as lupus.

STAR★METHODS

Detailed methods are provided in the online version of this paper and include the following:

- KEY RESOURCES TABLE
- RESOURCE AVAILABILITY
  - Lead contact
  - Materials availability
  - Data and code availability
- EXPERIMENTAL MODEL AND STUDY PARTICIPANT DETAILS
  - Human subjects
  - Human primary cell culture
- METHOD DETAILS
  - Cell culture and stimulations
  - Accell siRNA-based knockdown
  - Knockout keratinocyte generation using CRISPR/Cas9
  - Stable MX1 reporter line generation
  - Western blot analysis

- Gene expression analysis
- Flow cytometry
- Microarray
- Bulk RNA sequencing
- Transient transfections
- HERC6 over-expressing keratinocytes
- Immunoprecipitation assay
- Immunofluorescence staining

- QUANTIFICATION AND STATISTICAL ANALYSIS

SUPPLEMENTAL INFORMATION

Supplemental information can be found online at https://doi.org/10.1016/j.isci.2024.108986.

ACKNOWLEDGMENTS

This work was supported by the National Institute of Arthritis and Musculoskeletal and Skin 779 Disease of the NIH under award numbers R21-AR077741 (J.E.G.), P30-AR075043 (J.E.G.), R01-780 AI130025 (J.E.G.), the A. Alfred Taubman Medical Research Institute (J.E.G.), R01-AR071384 (J.M.K.), R01-AR081640 (J.M.K.), and K24-AR076975 (J.M.K.).

AUTHOR CONTRIBUTIONS

R.U. and J.E.G. conceptualized the current study. R.U., M.K.S., K.Z.Y., P.V., O.P., and M.G.K. performed experiments and analyzed data. R.U. generated the HERC6 knockout and over-expressing keratinocytes. F.M., R.W., W.R.S., E.M., A.C.B., and L.C.T. analyzed the bulk RNA-seq and scRNA-seq data. R.U. and J.E.G. wrote the original manuscript. J.M.K. and J.E.G. contributed by providing supervision. All the authors contributed by reviewing the manuscript.

DECLARATION OF INTERESTS

The authors declare no competing interests.

Received: September 21, 2023
Revised: November 10, 2023
Accepted: January 17, 2024
Published: January 23, 2024

REFERENCES

1. Sirobhushanam, S., Lazar, S., and Kahlenberg, J.M. (2021). Interferons in Systemic Lupus Erythematosus. Rheum. Dis. Clin. N. Am. *47*, 297–315. https://doi.org/10.1016/j.rdc.2021.04.001.
2. Xing, E., Billi, A.C., and Gudjonsson, J.E. (2022). Sex Bias and Autoimmune Diseases. J. Invest. Dermatol. *142*, 857–866. https://doi.org/10.1016/j.jid.2021.06.008.
3. Sontheimer, R.D. (1997). The lexicon of cutaneous lupus erythematosus–a review and personal perspective on the nomenclature and classification of the cutaneous manifestations of lupus erythematosus. Lupus *6*, 84–95. https://doi.org/10.1177/096120339700600203.
4. Stannard, J.N., Reed, T.J., Myers, E., Lowe, L., Sarkar, M.K., Xing, X., Gudjonsson, J.E., and Kahlenberg, J.M. (2017). Lupus Skin Is Primed for IL-6 Inflammatory Responses through a Keratinocyte-Mediated Autocrine Type I Interferon Loop. J. Invest. Dermatol. *137*, 115–122. https://doi.org/10.1016/j.jid.2016.09.008.
5. Sarkar, M.K., Hile, G.A., Tsoi, L.C., Xing, X., Liu, J., Liang, Y., Berthier, C.C., Swindell, W.R., Patrick, M.T., Shao, S., et al. (2018). Photosensitivity and type I IFN responses in cutaneous lupus are driven by epidermal-derived interferon kappa. Ann. Rheum. Dis. *77*, 1653–1664. https://doi.org/10.1136/annrheumdis-2018-213197.
6. Sarkar, M.K., Uppala, R., Zeng, C., Billi, A.C., Tsoi, L.C., Kidder, A., Xing, X., Perez White, B.E., Shao, S., Plazyo, O., et al. (2023). Keratinocytes sense and eliminate CRISPR DNA through STING/IFN-kappa activation and APOBEC3G induction. J. Clin. Invest. *133*, e159393. https://doi.org/10.1172/JCI159393.
7. Decout, A., Katz, J.D., Venkatraman, S., and Ablasser, A. (2021). The cGAS-STING pathway as a therapeutic target in inflammatory diseases. Nat. Rev. Immunol. *21*, 548–569. https://doi.org/10.1038/s41577-021-00524-z.
8. Kemp, M.G., Lindsey-Boltz, L.A., and Sancar, A. (2015). UV Light Potentiates STING (Stimulator of Interferon Genes)-dependent Innate Immune Signaling through Deregulation of ULK1 (Unc51-like Kinase 1). J. Biol. Chem. *290*, 12184–12194. https://doi.org/10.1074/jbc.M115.649301.
9. Sun, L., Wu, J., Du, F., Chen, X., and Chen, Z.J. (2013). Cyclic GMP-AMP synthase is a cytosolic DNA sensor that activates the type I interferon pathway. Science *339*, 786–791. https://doi.org/10.1126/science.1232458.
10. Dobbs, N., Burnaevskiy, N., Chen, D., Gonugunta, V.K., Alto, N.M., and Yan, N. (2015). STING Activation by Translocation from the ER Is Associated with Infection and Autoinflammatory Disease. Cell Host Microbe *18*, 157–168. https://doi.org/10.1016/j.chom.2015.07.001.
11. Tsoi, L.C., Hile, G.A., Berthier, C.C., Sarkar, M.K., Reed, T.J., Liu, J., Uppala, R., Patrick, M., Raja, K., Xing, X., et al. (2019). Hypersensitive IFN Responses in Lupus Keratinocytes Reveal Key Mechanistic Determinants in Cutaneous. J. Immunol. *202*, 2121–2130. https://doi.org/10.4049/jimmunol.1800650.
12. Isaacs, A., and Lindenmann, J. (1957). Virus interference. I. The interferon. Proc. R. Soc. Lond. B Biol. Sci. *147*, 258–267. https://doi.org/10.1098/rspb.1957.0048.
13. Wang, W., Xu, L., Su, J., Peppelenbosch, M.P., and Pan, Q. (2017). Transcriptional Regulation of Antiviral Interferon-Stimulated Genes. Trends Microbiol. *25*, 573–584. https://doi.org/10.1016/j.tim.2017.01.001.
14. Ma, F., Li, B., Yu, Y., Iyer, S.S., Sun, M., and Cheng, G. (2015). Positive feedback regulation of type I interferon by the interferon-stimulated gene STING. EMBO Rep. *16*, 202–212. https://doi.org/10.15252/embr.201439366.
15. Kong, L., Sui, C., Chen, T., Zhang, L., Zhao, W., Zheng, Y., Liu, B., Cheng, X., and Gao, C.

(2023). The ubiquitin E3 ligase TRIM10 promotes STING aggregation and activation in the Golgi apparatus. Cell Rep. *42*, 112306. https://doi.org/10.1016/j.celrep.2023.112306.

16. Cui, Y., Yu, H., Zheng, X., Peng, R., Wang, Q., Zhou, Y., Wang, R., Wang, J., Qu, B., Shen, N., et al. (2017). SENP7 Potentiates cGAS Activation by Relieving SUMO-Mediated Inhibition of Cytosolic DNA Sensing. PLoS Pathog. *13*, e1006156. https://doi.org/10.1371/journal.ppat.1006156.
17. Liu, S., Cai, X., Wu, J., Cong, Q., Chen, X., Li, T., Du, F., Ren, J., Wu, Y.T., Grishin, N.V., and Chen, Z.J. (2015). Phosphorylation of innate immune adaptor proteins MAVS, STING, and TRIF induces IRF3 activation. Science *347*, aaa2630. https://doi.org/10.1126/science.aaa2630.
18. Zhao, D., Gao, Y., Su, Y., Zhou, Y., Yang, T., Li, Y., Wang, Y., Sun, Y., Chen, L., Zhang, F., et al. (2023). Oroxylin A regulates cGAS DNA hypermethylation induced by methionine metabolism to promote HSC senescence. Pharmacol. Res. *187*, 106590. https://doi.org/10.1016/j.phrs.2022.106590.
19. Chen, G., Yan, Q., Liu, L., Wen, X., Zeng, H., and Yin, S. (2022). Histone Deacetylase 3 Governs beta-Estradiol-ERalpha-Involved Endometrial Tumorigenesis via Inhibition of STING Transcription. Cancers *14*, 4718. https://doi.org/10.3390/cancers14194718.
20. Jacquet, S., Pontier, D., and Etienne, L. (2020). Rapid Evolution of HERC6 and Duplication of a Chimeric HERC5/6 Gene in Rodents and Bats Suggest an Overlooked Role of HERCs in Mammalian Immunity. Front. Immunol. *11*, 605270. https://doi.org/10.3389/fimmu.2020.605270.
21. Dong, Z., Yan, Q., Cao, W., Liu, Z., and Wang, X. (2022). Identification of key molecules in COVID-19 patients significantly correlated with clinical outcomes by analyzing transcriptomic data. Front. Immunol. *13*, 930866. https://doi.org/10.3389/fimmu.2022.930866.
22. Zhong, Y., Zhang, W., Hong, X., Zeng, Z., Chen, Y., Liao, S., Cai, W., Xu, Y., Wang, G., Liu, D., et al. (2022). Screening Biomarkers for Systemic Lupus Erythematosus Based on Machine Learning and Exploring Their Expression Correlations With the Ratios of Various Immune Cells. Front. Immunol. *13*, 873787. https://doi.org/10.3389/fimmu.2022.873787.
23. Oudshoorn, D., van Boheemen, S., Sánchez-Aparicio, M.T., Rajsbaum, R., García-Sastre, A., and Versteeg, G.A. (2012). HERC6 is the main E3 ligase for global ISG15 conjugation in mouse cells. PLoS One *7*, e29870. https://doi.org/10.1371/journal.pone.0029870.
24. Karnell, J.L., Wu, Y., Mittereder, N., Smith, M.A., Gunsior, M., Yan, L., Casey, K.A., Henault, J., Riggs, J.M., Nicholson, S.M., et al. (2021). Depleting plasmacytoid dendritic cells reduces local type I interferon responses and disease activity in patients with cutaneous lupus. Sci. Transl. Med. *13*, eabf8442. https://doi.org/10.1126/scitranslmed.abf8442.
25. Berghöfer, B., Frommer, T., Haley, G., Fink, L., Bein, G., and Hackstein, H. (2006). TLR7 ligands induce higher IFN-alpha production in females. J. Immunol. *177*, 2088–2096. https://doi.org/10.4049/jimmunol.177.4.2088.
26. Meier, A., Chang, J.J., Chan, E.S., Pollard, R.B., Sidhu, H.K., Kulkarni, S., Wen, T.F., Lindsay, R.J., Orellana, L., Mildvan, D., et al. (2009). Sex differences in the Toll-like receptor-mediated response of plasmacytoid dendritic cells to HIV-1. Nat. Med. *15*, 955–959. https://doi.org/10.1038/nm.2004.
27. Staeheli, P., Haller, O., Boll, W., Lindenmann, J., and Weissmann, C. (1986). Mx protein: constitutive expression in 3T3 cells transformed with cloned Mx cDNA confers selective resistance to influenza virus. Cell *44*, 147–158. https://doi.org/10.1016/0092-8674(86)90493-9.
28. Buljan, M., Ciuffa, R., van Drogen, A., Vichalkovski, A., Mehnert, M., Rosenberger, G., Lee, S., Varjosalo, M., Pernas, L.E., Spegg, V., et al. (2020). Kinase Interaction Network Expands Functional and Disease Roles of Human Kinases. Mol. Cell *79*, 504–520.e9. https://doi.org/10.1016/j.molcel.2020.07.001.
29. Zou, R., Xu, Y., Feng, Y., Shen, M., Yuan, F., and Yuan, Y. (2020). YAP nuclear-cytoplasmic translocation is regulated by mechanical signaling, protein modification, and metabolism. Cell Biol. Int. *44*, 1416–1425. https://doi.org/10.1002/cbin.11345.
30. Stein, C., Bardet, A.F., Roma, G., Bergling, S., Clay, I., Ruchti, A., Agarinis, C., Schmelzle, T., Bouwmeester, T., Schübeler, D., and Bauer, A. (2015). YAP1 Exerts Its Transcriptional Control via TEAD-Mediated Activation of Enhancers. PLoS Genet. *11*, e1005465. https://doi.org/10.1371/journal.pgen.1005465.
31. Kastan, N., Gnedeva, K., Alisch, T., Petelski, A.A., Huggins, D.J., Chiaravalli, J., Aharanov, A., Shakked, A., Tzahor, E., Nagiel, A., et al. (2021). Small-molecule inhibition of Lats kinases may promote Yap-dependent proliferation in postmitotic mammalian tissues. Nat. Commun. *12*, 3100. https://doi.org/10.1038/s41467-021-23395-3.
32. Hochrainer, K., Mayer, H., Baranyi, U., Binder, B., Lipp, J., and Kroismayr, R. (2005). The human HERC family of ubiquitin ligases: novel members, genomic organization, expression profiling, and evolutionary aspects. Genomics *85*, 153–164. https://doi.org/10.1016/j.ygeno.2004.10.006.
33. Billi, A.C., Gharaee-Kermani, M., Fullmer, J., Tsoi, L.C., Hill, B.D., Gruszka, D., Ludwig, J., Xing, X., Estadt, S., Wolf, S.J., et al. (2019). The female-biased factor VGLL3 drives cutaneous and systemic autoimmunity. JCI Insight *4*, e127291. https://doi.org/10.1172/jci.insight.127291.
34. Hori, N., Okada, K., Takakura, Y., Takano, H., Yamaguchi, N., and Yamaguchi, N. (2020). Vestigial-like family member 3 (VGLL3), a cofactor for TEAD transcription factors, promotes cancer cell proliferation by activating the Hippo pathway. J. Biol. Chem. *295*, 8798–8807. https://doi.org/10.1074/jbc.RA120.012781.
35. Figeac, N., Mohamed, A.D., Sun, C., Schönfelder, M., Matallanas, D., Garcia-Munoz, A., Missiaglia, E., Collie-Duguid, E., De Mello, V., Pobbati, A.V., et al. (2019). VGLL3 operates via TEAD1, TEAD3 and TEAD4 to influence myogenesis in skeletal muscle. J. Cell Sci. *132*, jcs225946. https://doi.org/10.1242/jcs.225946.
36. Liang, Y., Tsoi, L.C., Xing, X., Beamer, M.A., Swindell, W.R., Sarkar, M.K., Berthier, C.C., Stuart, P.E., Harms, P.W., Nair, R.P., et al. (2017). A gene network regulated by the transcription factor VGLL3 as a promoter of sex-biased autoimmune diseases. Nat. Immunol. *18*, 152–160. https://doi.org/10.1038/ni.3643.
37. Yuan, L., Mao, Y., Luo, W., Wu, W., Xu, H., Wang, X.L., and Shen, Y.H. (2017). Palmitic acid dysregulates the Hippo-YAP pathway and inhibits angiogenesis by inducing mitochondrial damage and activating the cytosolic DNA sensor cGAS-STING-IRF3 signaling mechanism. J. Biol. Chem. *292*, 15002–15015. https://doi.org/10.1074/jbc.M117.804005.
38. Sladitschek-Martens, H.L., Guarnieri, A., Brumana, G., Zanconato, F., Battilana, G., Xiccato, R.L., Panciera, T., Forcato, M., Bicciato, S., Guzzardo, V., et al. (2022). YAP/TAZ activity in stromal cells prevents ageing by controlling cGAS-STING. Nature *607*, 790–798. https://doi.org/10.1038/s41586-022-04924-6.
39. Moroishi, T., Hayashi, T., Pan, W.W., Fujita, Y., Holt, M.V., Qin, J., Carson, D.A., and Guan, K.L. (2016). The Hippo Pathway Kinases LATS1/2 Suppress Cancer Immunity. Cell *167*, 1525–1539.e17. https://doi.org/10.1016/j.cell.2016.11.005.
40. Niewold, T.B., Adler, J.E., Glenn, S.B., Lehman, T.J.A., Harley, J.B., and Crow, M.K. (2008). Age- and sex-related patterns of serum interferon-alpha activity in lupus families. Arthritis Rheum. *58*, 2113–2119. https://doi.org/10.1002/art.23619.
41. Congy-Jolivet, N., Cenac, C., Dellacasagrande, J., Puissant-Lubrano, B., Apoil, P.A., Guedj, K., Abbas, F., Laffont, S., Sourdet, S., Guyonnet, S., et al. (2022). Monocytes are the main source of STING-mediated IFN-alpha production. EBioMedicine *80*, 104047. https://doi.org/10.1016/j.ebiom.2022.104047.
42. Billi, A.C., Ma, F., Plazyo, O., Gharaee-Kermani, M., Wasikowski, R., Hile, G.A., Xing, X., Yee, C.M., Rizvi, S.M., Maz, M.P., et al. (2022). Nonlesional lupus skin contributes to inflammatory education of myeloid cells and primes for cutaneous inflammation. Sci. Transl. Med. *14*, eabn2263. https://doi.org/10.1126/scitranslmed.abn2263.
43. Psarras, A., Alase, A., Antanaviciute, A., Carr, I.M., Md Yusof, M.Y., Wittmann, M., Emery, P., Tsokos, G.C., and Vital, E.M. (2020). Functionally impaired plasmacytoid dendritic cells and non-haematopoietic sources of type I interferon characterize human autoimmunity. Nat. Commun. *11*, 6149. https://doi.org/10.1038/s41467-020-19918-z.
44. Cao, L., Zhang, H., Bai, J., Wu, T., Wang, Y., Wang, N., and Huang, C. (2022). HERC6 is upregulated in peripheral blood mononuclear cells of patients with systemic lupus erythematosus and promotes the disease progression. Autoimmunity *55*, 506–514. https://doi.org/10.1080/08916934.2022.2103800.
45. Qing, J., Song, W., Tian, L., Samuel, S.B., and Li, Y. (2022). Potential Small Molecules for Therapy of Lupus Nephritis Based on Genetic Effect and Immune Infiltration. BioMed Res. Int. *2022*, 2259164. https://doi.org/10.1155/2022/2259164.
46. Alexopoulou, L., Holt, A.C., Medzhitov, R., and Flavell, R.A. (2001). Recognition of double-stranded RNA and activation of NF-kappaB by Toll-like receptor 3. Nature *413*, 732–738. https://doi.org/10.1038/35099560.
47. Souyris, M., Cenac, C., Azar, P., Daviaud, D., Canivet, A., Grunenwald, S., Pienkowski, C., Chaumeil, J., Mejía, J.E., and Guéry, J.C. (2018). TLR7 escapes X chromosome inactivation in immune cells. Sci. Immunol. *3*, eaap8855. https://doi.org/10.1126/sciimmunol.aap8855.

48. Torcia, M.G., Nencioni, L., Clemente, A.M., Civitelli, L., Celestino, I., Limongi, D., Fadigati, G., Perissi, E., Cozzolino, F., Garaci, E., and Palamara, A.T. (2012). Sex differences in the response to viral infections: TLR8 and TLR9 ligand stimulation induce higher IL10 production in males. PLoS One *7*, e39853. https://doi.org/10.1371/journal.pone.0039853.

49. Swindell, W.R., Stuart, P.E., Sarkar, M.K., Voorhees, J.J., Elder, J.T., Johnston, A., and Gudjonsson, J.E. (2014). Cellular dissection of psoriasis for transcriptome analyses and the post-GWAS era. BMC Med. Genom. *7*, 27. https://doi.org/10.1186/1755-8794-7-27.

50. Hile, G.A., Coit, P., Xu, B., Victory, A.M., Gharaee-Kermani, M., Estadt, S.N., Maz, M.P., Martens, J.W.S., Wasikowski, R., Dobry, C., et al. (2023). Regulation of Photosensitivity by the Hippo Pathway in Lupus Skin. Arthritis Rheumatol. *75*, 1216–1228. https://doi.org/10.1002/art.42460.

51. Swindell, W.R., Sarkar, M.K., Liang, Y., Xing, X., Baliwag, J., Elder, J.T., Johnston, A., Ward, N.L., and Gudjonsson, J.E. (2017). RNA-seq identifies a diminished differentiation gene signature in primary monolayer keratinocytes grown from lesional and uninvolved psoriatic skin. Sci. Rep. *7*, 18045. https://doi.org/10.1038/s41598-017-18404-9.

52. Rittié, L., and Fisher, G.J. (2005). Isolation and culture of skin fibroblasts. Methods Mol. Med. *117*, 83–98. https://doi.org/10.1385/1-59259-940-0:083.

53. Dickson, M.A., Hahn, W.C., Ino, Y., Ronfard, V., Wu, J.Y., Weinberg, R.A., Louis, D.N., Li, F.P., and Rheinwald, J.G. (2000). Human keratinocytes that express hTERT and also bypass a p16(INK4a)-enforced mechanism that limits life span become immortal yet retain normal growth and differentiation characteristics. Mol. Cell Biol. *20*, 1436–1447. https://doi.org/10.1128/MCB.20.4.1436-1447.2000.

54. Swindell, W.R., Beamer, M.A., Sarkar, M.K., Loftus, S., Fullmer, J., Xing, X., Ward, N.L., Tsoi, L.C., Kahlenberg, M.J., Liang, Y., and Gudjonsson, J.E. (2018). RNA-Seq Analysis of IL-1B and IL-36 Responses in Epidermal Keratinocytes Identifies a Shared MyD88-Dependent Gene Signature. Front. Immunol. *9*, 80. https://doi.org/10.3389/fimmu.2018.00080.

STAR★METHODS

KEY RESOURCES TABLE

REAGENT or RESOURCE	SOURCE	IDENTIFIER
Antibodies		
Human STAT1	Cell Signaling Technology	9172S
Human P-STAT1	Cell Signaling Technology	9167S
Human STAT2	Cell Signaling Technology	72604S
Human P-STAT2	Cell Signaling Technology	4441S
Human IRF3	Cell Signaling Technology	4302S
Human P-IRF3	Cell Signaling Technology	37829S
Human TBK1	Cell Signaling Technology	38066S
Human P-TBK1	Cell Signaling Technology	5483S
Human STING	Cell Signaling Technology	13647
Human P-STING	Cell Signaling Technology	19781
Human LATS1/2	Invitrogen	BS-4081R
Human P-LATS1/2	Invitrogen	PA5-64591
Human YAP	Cell Signaling Technology	8418S
Human P-YAP	Cell Signaling Technology	913008S
Human ACTIN	Cell Signaling Technology	8457S
Human HERC6	Thermo Fisher Scientific	PA5-57426
Human STING	Thermo Fisher Scientific	PA5-26751
Human LATS2	Thermo Fisher Scientific	17H14L2
HRP conjugated secondary	CST	58802S & 93702S
Fluorochrome conjugated secondary antibodies	Fisher Scientific	A-11008 & A8_2340767
Chemicals, peptides, and recombinant proteins		
HERC6 siRNA	Dharmacon	E-005175
TMEM siRNA	Dharmacon	E-024333
LATS2 siRNA	Dharmacon	E-003865
Non-targeting control siRNA	Dharmacon	D-001910-01-05
siRNA Buffer	Dharmacon	B-002000-UB-100
siRNA Delivery media	Dharmacon	B-005000
TransfeX	ATCC	ACS4005
Pierce RIPA buffer	ThermoFisher Scientific	89900
Protease and phosphatase inhibitor cocktail	Sigma	36978
Taqman Universal PCR Master MIx	ThermoFisher Scientific	4304437
Turbofectin	Origene	TF8100
Lipofectamine 3000	ThermoFisher Scientific	L3000001
Polybrene	Sigma Aldrich	TR-1003-G
Magnetic Protein A/G beads	ThermoFisher Scientific	88803
TRIS-Glycine gels	Bio-Rad	456-1094S
ECL substrate	Stellar Scientific	MMZR-XR96
RNeasy plus kit	Qiagen	74136
Recombinant Human IFN-α	PBI assay	11100-1
cGAMP	Invivogen	Tlrl-nacga23

(*Continued on next page*)

Continued

REAGENT or RESOURCE	SOURCE	IDENTIFIER
TLR3 agonist	Invivogen	tlrl-pic
E. coli	ThermoFisher Scientific	C737303
CRISPR/Cas9 backbone	Addgene	48138
Promoterless lentiviral vector	abm	ABM-LV059
CMV promoter-driven GFP lentiviral vector	abm	ABM-LV011-a
HERC6 Human tagged ORF	Origene	RC218907
DYK-HERC6	Genscript	SC1626
Myc-LATS2	Addgene	66852
Keratinocyte Serum Free medium	ThermoFisher Scientific	17005-042
Medium 154	ThermoFisher Scientific	M154500
Opti-MEM	GIBCO	31985–070
Dulbecco's modified Eagle's medium	ThermoFisher Scientific	11320033
Deposited data		
Bulk RNA-sequencing data	In this paper	GEO: GSE253221
Primary keratinocytes microarray data	Swindell et al. 2014[49]	GEO: GSE7216, GSE18590, GSE21364, GSE21567, GSE27186, GSE30355, GSE32685, GSE33495, GSE33536, GSE34528, GSE36222, GSE36287 and GSE37637

RESOURCE AVAILABILITY

Lead contact

For additional details and inquiries regarding resources and reagents, please contact the lead author, Johann E. Gudjonsson (johanng@med.umich.edu).

Materials availability

Knockout cell lines, guide RNAs, and plasmids generated in this study are available upon request.

Data and code availability

- The data in the present study can be obtained from the public datasets specified in the key resources table.
- This paper does not include the original code.
- Any additional information will be available upon request from the lead author.

EXPERIMENTAL MODEL AND STUDY PARTICIPANT DETAILS

Human subjects

SLE patients and healthy controls (Table S1) were recruited from the Taubman Institute Innovative Research Program Personalized Medicine through Integration of Immune Phenotypes in Autoimmune Skin Disease (TIIP-PerMIPA cohort) as described in a previous study.[50] As per the principles of the Declaration of Helsinki, all patients and healthy controls gave written, informed consent before inclusion in the study.

Human primary cell culture

Human keratinocytes were obtained from SLE patients and healthy adults by following the procedure described in a previous study.[51] Skin biopsies were collected from volunteer patients in accordance with the University of Michigan institutional review board-approved protocols and with the subjects' informed consent. The cultures were maintained using serum-free medium and were used for experimentation at passage 2 or 3 with a calcium concentration of 0.1 mM. Primary human dermal fibroblasts were isolated from human skin described in a previous study.[52]

METHOD DETAILS

Cell culture and stimulations

N/TERT human immortalized keratinocyte cell line was obtained from Dr. James G. Rheinwald and was used for performing gene knockdowns or knockout (KO) experiments.[53] These cells have demonstrated typical differentiation traits in monolayer and organotypic skin models.

N/TERTs or KOs were cultured in Keratinocyte Serum Free Medium (KSFM), which was enriched with 30 μg/ml bovine pituitary extract, 0.2 ng/ml epidermal growth factor, and 0.3 mM calcium chloride.[54] Cells were used for various experiments following the attainment of the appropriate confluency. Cells were deprived of growth factors for 24 hours before being exposed to recombinant human IFN-α. Complete growth media was used for cGAMP or TLR3 agonist stimulations. Total RNA or protein was isolated after indicated time points of stimulations or transfections.

Accell siRNA-based knockdown

Keratinocytes were seeded into 48-well plates and incubated overnight at 37°C with 5% CO2. A 100μM siRNA stock was prepared using siRNA buffer, diluted to 1μM siRNA using Accell siRNA delivery media, and added to each well. A non-targeting control siRNA was used for negative control. Total RNA was isolated after 48 hours of siRNA incubation. cGAMP or TLR3 agonist stimulations were performed after 48 hours of incubation with siRNA.

Knockout keratinocyte generation using CRISPR/Cas9

CRISPR KO keratinocytes were generated as previously described.[5] Briefly, the target single-guide RNA (sgRNA) was designed using a web interface developed explicitly for CRISPR design by the BROAD institute (https://portals.broadinstitute.org/gpp/public/analysis-tools/sgrna-design). The target sequences for synthetic sgRNA were integrated into a cloning backbone known as pSpCas9 (BB)_2A-GFP. Integrated sgRNA sequences into the plasmids were transformed using the competent *E. coli*. Verified plasmid DNA by Sanger sequencing was used to transfect the N/TERT cells using TransfeX. GFP-expressing cells were clonally expanded and sequenced to investigate the INDELs. *IFNK*, *TYK2*, *IFNB1*, and *STING* KO keratinocytes were generated as previously described.[5,6] *HERC6* KO keratinocytes were generated by annealing the following oligonucleotides: HERC6E1SG2F1: 5′-CACCGATTGTTGATCTCGTGAGCTG-3′ and HERC6E1SG2R1: 5′-AAACCAGCTCACGAGATCAACAATC-3′. Genotyping for HERC6 clones was performed with specific primers for HERC6: HERC6PCRF4: AAAGTGCTGTCTTAAACTTGTGT and HERC6PCRR4: TTGAATAAATGAAGGAGTGGGTTGA.

Stable MX1 reporter line generation

A 2nd generation promoterless lentiviral vector carrying a puromycin selection marker was purchased from abm which contains a multiple cloning site (MCS) upstream of GFP. The MX1 promoter region of 991bps upstream of the transcription start site was cloned into MCS using the EcoRI and XbaI restriction sites. Agarose gels and sanger sequencing confirmed MX1 cloning into the lentiviral backbone vector. HEK293T cells were used for packaging and generating viral particles. Viral particles generated were collected after 48hrs of transfection and immediately used to transduce the keratinocytes at a multiplicity of infection (MOI) of 1. The transduced keratinocytes were expanded in a selection medium containing 10ug/ml puromycin for 5 days or until all the un-transduced cells were dead. Puromycin concentration of 10ug/ml was determined after performing a drug kill curve in keratinocytes. CMV promoter-driven GFP or promoterless empty vectors were used as controls. Single-cell sorted transduced keratinocytes were expanded, and validation experiments were performed to choose an optimum clone.

Western blot analysis

Total protein was extracted from the cells using Pierce RIPA buffer supplemented with protease and phosphatase inhibitor cocktail. 20ug of total protein samples were then subjected to electrophoresis on pre-cast TRIS-Glycine gels. After blocking with 5% BSA, the membrane was probed with primary antibodies, followed by HRP conjugated secondary antibodies. Membranes were washed three times and were imaged on iBright using the ECL substrate. All experiments were performed at least three times with similar results.

Gene expression analysis

Total RNA was harvested from cells using Qiagen RNeasy plus kit. qRT-PCR was performed on a 7900HT Fast Real-time PCR system (AppliedBiosystems) using TaqMan Universal PCR Master Mix, and RPLP0 was used as endogenous control.

Flow cytometry

Single-cell suspension was prepared from untransduced, CMVGFP, and MX1GFP transduced keratinocytes. Live cells were first gated manually to exclude dead cells or debris, and GFP-expressing cells were gated based on CMVGFP transduced cells which constitutively expressed stable GFP on a BD LSR II (BD Biosciences). Data were analyzed using FlowJo software.

Microarray

MX1-correlated genes were identified by evaluating gene expression across 118 keratinocyte (KC) microarray samples curated by Swindell et al.[49] The 118 samples had been generated using the same commercial microarray platform (Affymetrix Human Genome Plus 2.0 array) and were compiled from 13 Gene Expression Omnibus series submissions (GSE7216, GSE18590, GSE21364, GSE21567, GSE27186, GSE30355, GSE32685, GSE33495, GSE33536, GSE34528, GSE36222, GSE36287 and GSE37637). Microarray samples were generated using RNA from cultured KCs following various forms of treatment (e.g., genetic mutations, siRNA knockdown, cytokines). The expression of *MX1* was detected ($P < 0.05$) with respect to 94 of the 118 microarray samples (79.7%). Genes most strongly correlated with *MX1* expression

included interferon induced protein 44 (*IFI44*), interferon induced protein with tetratricopeptide repeats 1 (*IFIT1*), interferon induced protein 44 like (*IFI44L*), and HECT and RLD domain containing E3 ubiquitin protein ligase family member 6 (*HERC6*).

Bulk RNA sequencing

Bulk RNAseq for control or HERC6 KD primary human keratinocytes with or without GAMP stimulation were performed (n=3 each group, and 3 male and 3 female keratinocytes were included per group). 150bp paired-ended reads were generated. The reads were adapter trimmed and aligned to the human genome hg19, with only the uniquely mapped reads used for expression level quantification. DESeq2 was used to perform read normalization and differential expression analyses. The data are available on GEO (Accession # GSE253221).

Transient transfections

Cells were transfected using Lipofectamine transfection reagent in Opti-MEM. Plasmid DNA (2 μg per 6-well dish or 1μg per 24-well dish) was diluted in Opti-MEM, lipofectamine, and p3000 reagent was separately diluted in Opti-MEM. After 5 min, the DNA was added to the p3000 mix and incubated at room temperature for 15 min. The mixed solution was pipetted dropwise into the medium, covering the adherent cells. Cells were transfected for 48hr before harvesting for downstream analysis.

HERC6 over-expressing keratinocytes

HERC6 over-expressing keratinocytes were generated by lentiviral transduction, like previously described [6]. Briefly, human HERC6 ORF-containing mammalian vectors were packaged using the packaging plasmids and turbofectin in HEK293T cells. A day before transduction, keratinocytes were plated in serum-free media and transduced with the virus with 8μg/ml of polybrene. After drug selection, surviving clones were obtained by limited dilution, and the OE clones were verified by western blotting.

Immunoprecipitation assay

HEK 293 cells were grown in Dulbecco's modified Eagle's medium with 10% fetal bovine serum. Cells were transfected using Lipofectamine 3000 with the DYK-HERC6 or Myc-LATS2 or both tagged cDNA constructs and harvested after 48 hours. 500μg total protein was incubated overnight with mono, or polyubiquitin conjugates antibody on a shaker at 4°C. Pierce Protein Magnetic Protein A/G beads were used to pull down immune complexes, which were then analyzed by western blotting.

Immunofluorescence staining

For *in vitro* studies, immunofluorescence staining was performed on cells plated on 8-well chamber slides. Cells were initially washed in ice-cold PBS, fixed in 4% PFA, blocked in BSA, and incubated with primary antibodies overnight at 4°C. The following day, cells were incubated for 1 hr in fluorochrome-conjugated secondary antibodies. Chamber slides were washed and prepared in mounting media with DAPI. Images were acquired using an inverted Zeiss microscope. Images presented are representative of at least three biological replicates.

QUANTIFICATION AND STATISTICAL ANALYSIS

Statistical testing was performed on data obtained from at least three independent experiments using GraphPad Prism version 9. Statistical significance was determined using Student's unpaired t-test or analysis of variance (ANOVA) as indicated in the legend ($*P < 0.05$, $**P < 0.01$, $***P < 0.001$, $****P < 0.0001$). After two-way ANOVA, Tukey's multiple comparison post hoc test was used with a 95% family-wise confidence level. Flow cytometry data were analyzed using FlowJo v10. The number of sampled units, n, is indicated in the figure legends and as data points on the bar plots. For microarray and bulk RNA-sequencing, a false discovery rate (FDR) of 0.05 was used to adjust and control for multiple testing.

iScience, Volume *27*

Supplemental information

HERC6 regulates STING activity in a sex-biased manner through modulation of LATS2/VGLL3 Hippo signaling

Ranjitha Uppala, Mrinal K. Sarkar, Kelly Z. Young, Feiyang Ma, Pritika Vemulapalli, Rachael Wasikowski, Olesya Plazyo, William R. Swindell, Emanual Maverakis, Mehrnaz Gharaee-Kermani, Allison C. Billi, Lam C. Tsoi, J. Michelle Kahlenberg, and Johann E. Gudjonsson

Figure S1

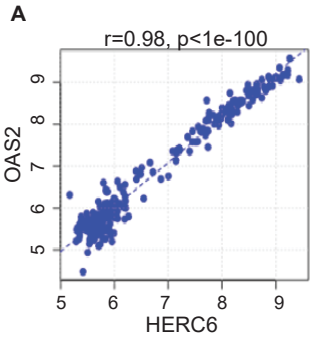

Figure S1. HERC6 correlation with OAS2. Related to Figure 1.
Correlation of *HERC6* mRNA expression with *OAS2* from primary human keratinocytes.

Figure S2

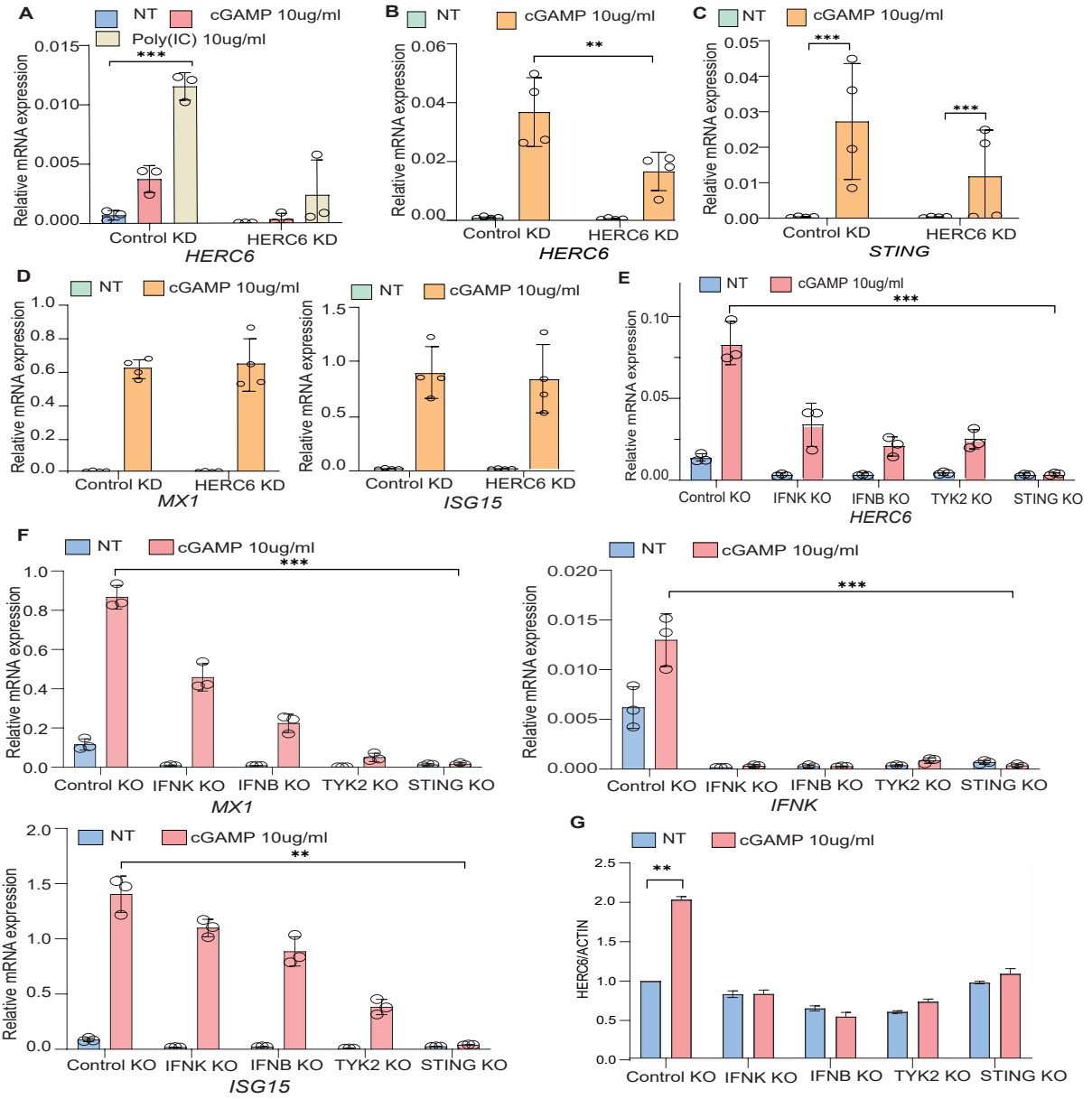

Figure S2. HERC6 activity in keratinocytes is STING-dependent. Related to Figure 2.

A. HERC6 knockdown efficiency in primary human keratinocytes (Mean +/P<0.01 = **, P<0.05 = *, ns = not significant, One-way ANOVA, n=3), and
B. HERC6 knockdown efficiency in primary human fibroblasts (Mean +/P<0.01 = **, P<0.05 = *, ns = not significant, One-way ANOVA, n=4)
C. Gene expression analysis of STING in primary human fibroblasts (Mean +/***, P<0.01 = **, P<0.05 = *, ns = not significant, Student's t-test, n=3)
D. Gene expression analysis of ISGs in cGAMP stimulated control or human fibroblasts (Mean +/- SEM, P<0.001 = ***, P<0.01 = **, P<0.05 = *, ns = not significant, Student's t-test, n=4). Assume that NT = no treatment group.
E. HERC6 gene expression in indicated knockout keratinocytes (Mean +/P<0.01 = **, P<0.05 = *, ns = not significant, One-way ANOVA, n=3). Assume that NT = no treatment group.
F. Gene expression analysis of ISGs cGAMP stimulated control or(Mean +/- SEM, P<0.001 = ***, P<0.01 = **, P<0.05 = *, ns = not significant, n=3)
G. Quantification of western blot from Figure 2D representing normalized relative band intensity of HERC6 (Mean +/- SEM, P<0.001 = ***, P<0.01 = **, P<0.05 = *, ns = not significant, Student's t-test, n=3). Assume that NT = no treatment group.

Figure S3

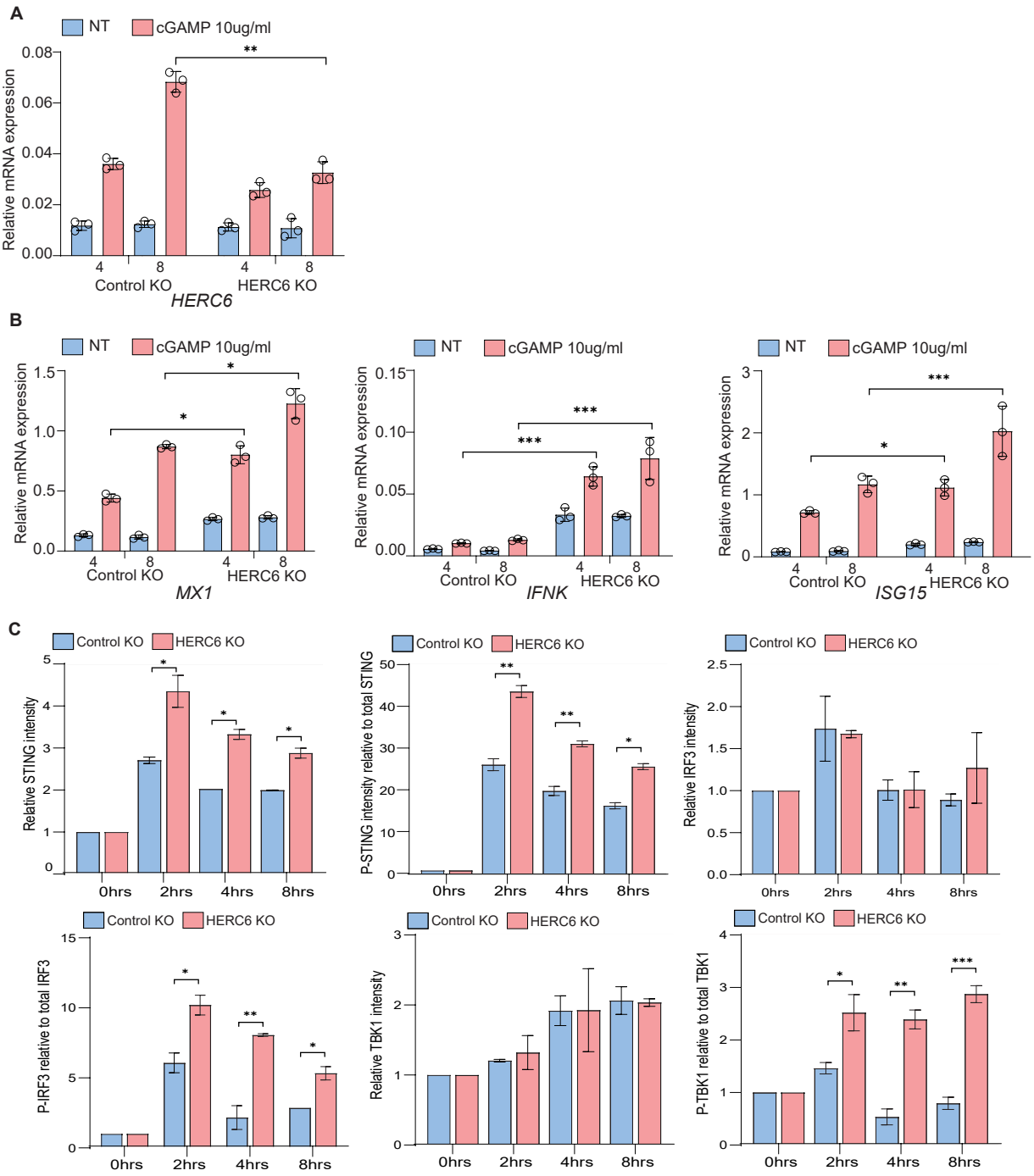

Figure S3. HERC6 knockout keratinocytes have increased STING activity upon cGAMP stimulation. Related to Figure 3.

A. HERC6 expression by qPCR in indicated knockout keratinocytes (Mean +/- SEM, P<0.001 = ***, P<0.01 = **, P<0.05 = *, ns = not significant, One-way ANOVA, n=3)

B. Gene expression analysis for ISGs in cGAMP stimulated control or HERC6 knockout keratinocytes at indicated time points (Mean +/- SEM, P<0.001 = ***, P<0.01 = **, P<0.05 = *, ns = not significant, Two-way ANOVA, n=3). Assume that NT = no treatment group.

C. Quantification of western blot from Figure 3C representing normalized relative band intensity of STING, P-STING, IRF3, P-IRF3, TBK1 & P-TBK1 (Mean +/- SEM, P<0.001 = ***, P<0.01 = **, P<0.05 = *, ns = not significant, Two-way ANOVA, n=3). Assume that NT = no treatment group.

Figure S4

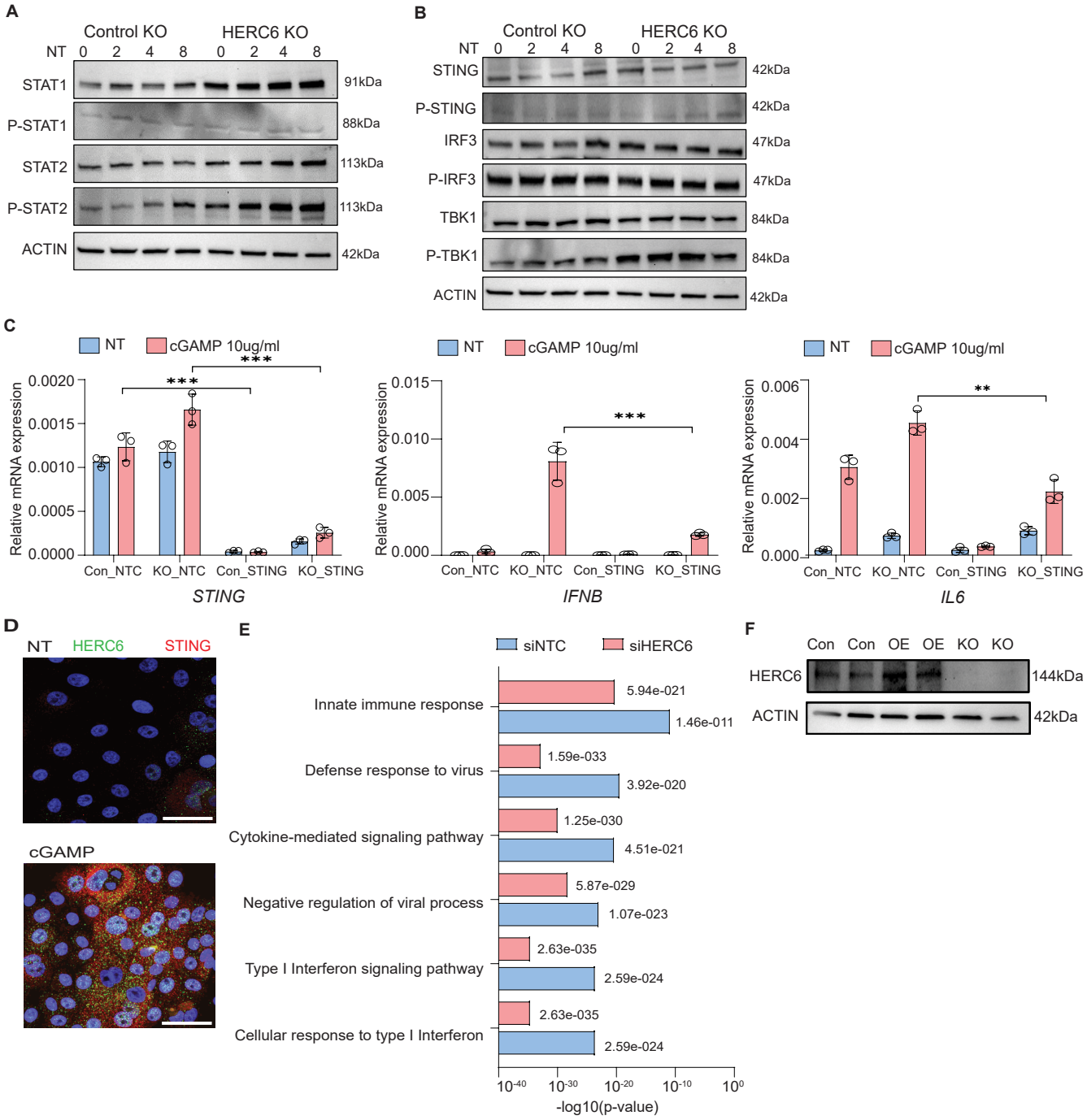

Figure S4. Sustained STING signaling activity in HERC6 knockout keratinocytes is dampened by STING inhibition. Related to Figure 3.

A. Western blot analysis of type I interferon-related genes in untreated control or *HERC6*knockout keratinocytes at indicated time points

B. Western blot analysis of STING pathway-related genes in untreated control or *HERC6*knockout keratinocytes at indicated time points

C. Gene expression analysis for STING-induced genes with or without *STING* knockdown in control or HERC6 knockout keratinocytes (Mean +/- SEM, P<0.001 = ***, P<0.01 = **, P<0.05 = *, ns = not significant, Two-way ANOVA, n=3). Assume that NT = no treatment group

D. Confocal image analysis of control keratinocytes with or without CGAMP (HERC6 in green, STING in red, and DAPI nuclear staining in blue)

E. GO terms biological processes for control knockdown (siNTC) and *HERC6* knockdown (*siHERC6*) primary human keratinocytes showing significance with cGAMP stimulation (FDRadjusted p-value of 0.05, n=3 males & 3 females)

F. Western blot analysis of control (Con), HERC6 OE (OE) or *HERC6* KO (KO) keratinocytes

Figure S5

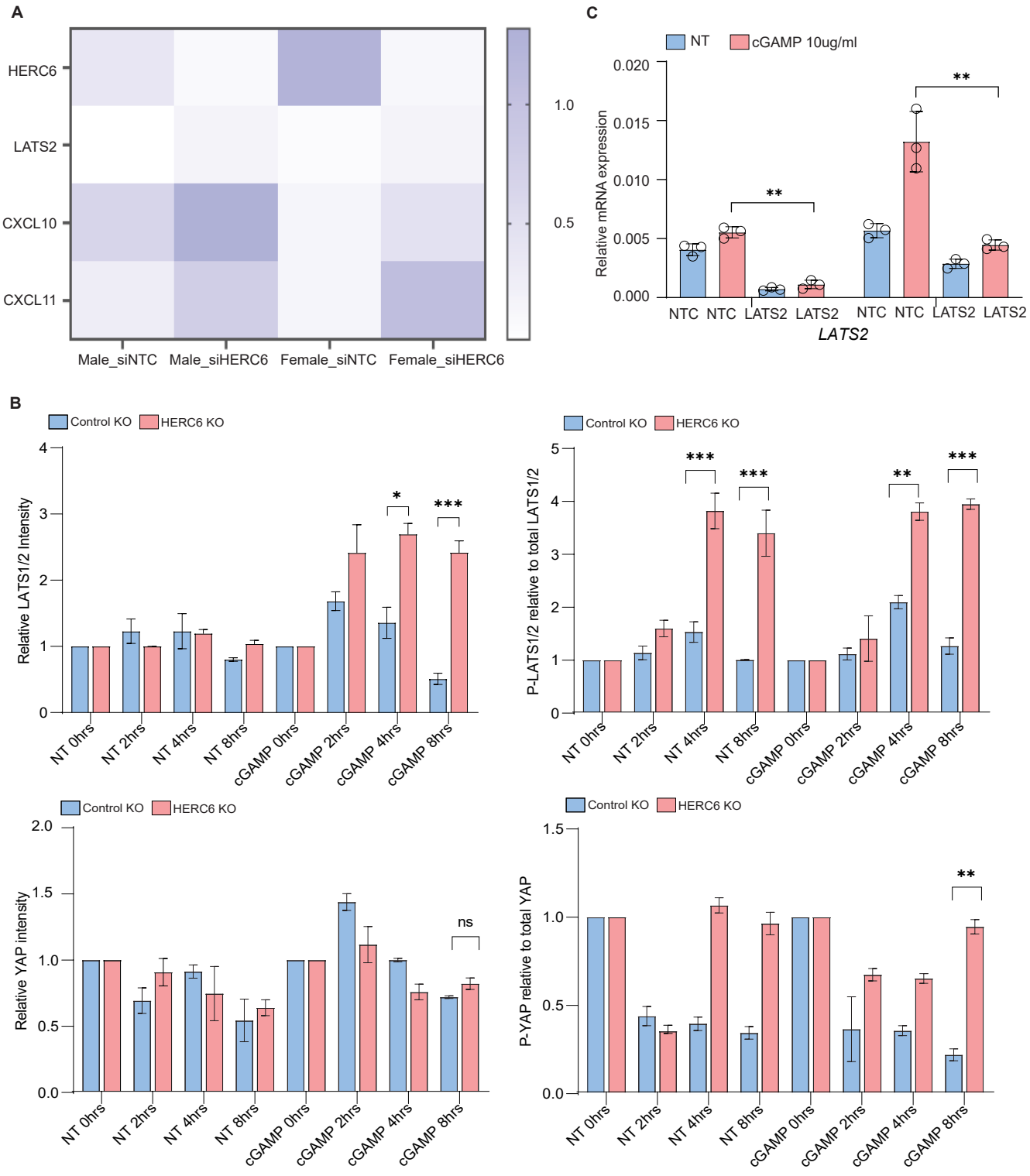

Figure S5. HERC6 knockout keratinocytes exhibit increased LATS2 activity. Related to Figure 4.
A. Heat map representing Log2 fold change of HERC6, LATS2, CXCL10, and CXCL11 in non- treated versus cGAMP stimulated control or HERC6 knockdown human primary keratinocytes through bulk RNA-sequencing
B. Quantification of western blot from Figure 4B representing normalized relative band intensity of LATS1/2, P-LATS1/2, YAP & P-YAP (Mean +/- SEM, P<0.001 = ***, P<0.01 = **, P<0.05 = *, ns = not significant, Two-way ANOVA, n=3). Assume that NT = no treatment group.
C. LATS2 knockdown efficiency by QPCR (Mean +/- SEM, P<0.001 = ***, P<0.01 = **, P<0.05 = *, ns = not significant, One-way ANOVA, n=3)

Figure S6

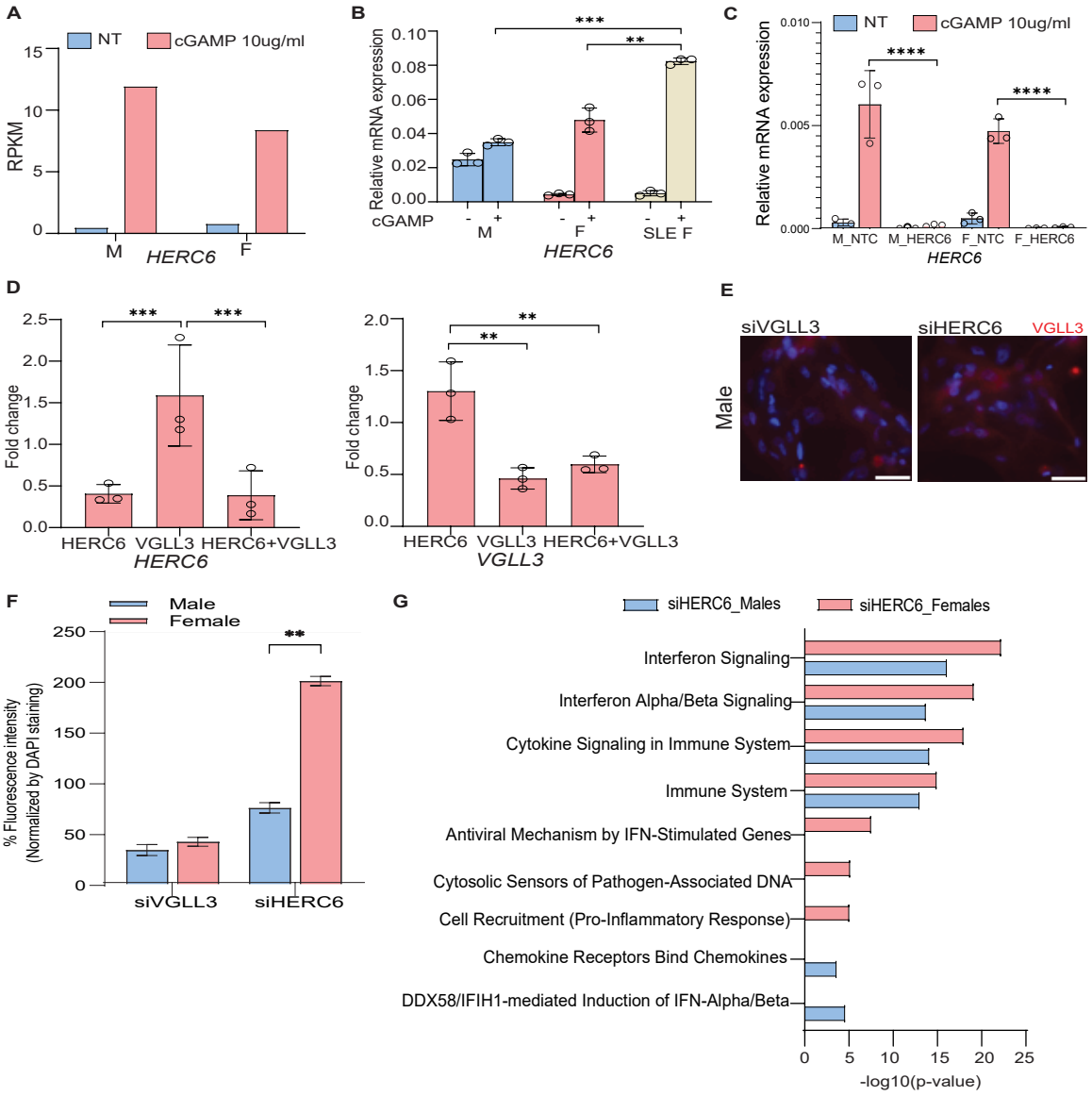

Figure S6. Negative regulatory role of HERC6 is female biased in keratinocytes. Related to Figure 6.
A. HERC6 expression in primary male (M) or female (F) keratinocytes stimulated with or without cGAMP
B. HERC6 gene expression in normal male (M), normal female (F), or SLE femalekeratinocytes with or without cGAMP stimulation (Mean +/- SEM, P<0.001 = ***, P<0.01 = **, P<0.05 = *, ns = not significant, Two-way ANOVA, n=3)
C. *HERC6* knockdown efficiency in primary human male (M) or Female (F) keratinocytescontrol (NTC) or HERC6 (HERC6) siRNA (Mean +/- SEM, P<0.001 = ***, P<0.01 = **, P<0.05 = *, ns = not significant, One-way ANOVA, n=3)
D. Gene expression analysis representing fold change compared to knockdown of noncontrol (NTC) of *HERC6*, *VGLL3*, or both *HERC6+VGLL3* in non-lesional female lupus keratinocytes (Mean +/- SEM, P<0.001 = ***, P<0.01 = **, P<0.05 = *, ns = not significant, Ordinary one-way ANOVA fold-change relative to control knockdown, n=3)
E. Immunofluorescence staining of VGLL3 in primary human male keratinocytes with VGLL3 or *HERC6* knockdown (VGLL3 in red & DAPI nuclear staining in blue)
F. Quantification of VGLL3 staining from Figure 6B & Supplemental Figure S6E representing % Fluorescence intensity normalized to DAPI staining (Mean +/- SEM, P<0.001 = ***, P<0.01 = **, P<0.05 = *, ns = not significant, Student's t-test, n=3)
G. GO terms for H*ERC6* knockdown (*siHERC6*) male or female keratinocytes showing significance with cGAMP stimulation ((FDR-adjusted p-value of 0.05, n=3)

Table S1: Study Participant Details. Related to STAR Methods.

Figure	Healthy controls		
Figures 3E, 3F, 6A & 6D	Age	Sex	Self-reported race/ethnicity
	48	Male	White, non-Hispanic
	34	Male	White, non-Hispanic
	36	Male	White, non-Hispanic
	46	Female	White, non-Hispanic
	41	Female	White, non-Hispanic
	36	Female	White, non-Hispanic
Figures 2A, 4A & 6B	50	Male	White, non-Hispanic
	36	Male	White, non-Hispanic
	67	Male	White, non-Hispanic
	39	Female	White, non-Hispanic
	19	Female	Black_White, non-Hispanic
	25	Female	White, non-Hispanic
Figure 6C	SLE patients		
	39	Female	White, non-Hispanic
	34	Female	White, non-Hispanic
	36	Female	White, non-Hispanic